CHEMMEDCHEM

DOI: 10.1002/cmdc.200700074

# Synthesis and Evaluation of 3-Phenylpyrazolo[3,4-*d*]pyrimidine-Peptide Conjugates as Src Kinase Inhibitors

Anil Kumar,[b] Yuehao Wang,[c] Xiaofeng Lin,[c] Gongqin Sun,[c] and Keykavous Parang*[a]

*3-Phenylpyrazolo[3,4-d]pyrimidine (PhPP) derivatives substituted with an alkyl or aryl carboxylic acid at the N1-endocyclic amine, such as PhPP-$CH_2$COOH ($IC_{50}$ = 250 μM), and peptides Ac-CIYKYY ($IC_{50}$ = 400 μM) and Ac-YIYGSFK ($IC_{50}$ = 570 μM) were weak inhibitors of poly$E_4$Y phosphorylation by active c-Src. A series of PhPP–peptide conjugates were synthesized using PhPP as an ATP mimic and CIYKYY or YIYGSFK as a peptide substrate to improve the inhibitory potency against active c-Src kinase. PhPP derivatives were attached to the N terminus or the side chain of amino acids in the peptide template. Two N-terminal substituted conjugates, PhPP-$CH_2$CO-CIYKYY ($IC_{50}$ = 0.38 μM) and PhPP-$CH_2$CO-YIYGSFK ($IC_{50}$ = 2.7 μM), inhibited the poly$E_4$Y phosphorylation by active c-Src significantly higher than that of the parent compounds. The conjugation of PhPP with the peptides produced a synergistic inhibition effect possibly through creation of favorable interactions between the conjugate and the kinase domain as shown by molecular modeling studies.*

## Introduction

Protein tyrosine kinases (PTKs) are enzymes that catalyze phosphorylation of tyrosine in many proteins by the transfer of the γ-phosphoryl group from ATP.[1] The Src family of protein tyrosine kinases (SFKs), Src, Yes, Lck, Fyn, Lyn, Fgr, Hck, Blk, and Yrk, are nonreceptor tyrosine kinases that have been implicated in the regulation of different cellular processes and in signal transduction pathways.[2,3] Src tyrosine kinases activity has been directly linked to cell growth, differentiation, and migration.[4]

Src, a prototypical member of SFKs, contributes significantly to cellular activation, adhesion, motility and survival, growth factor receptor signaling, and osteoclast activation.[5–9] Therefore, Src has been implicated in the development of inflammation-mediated bone loss and osteoporosis,[3,10,11] several different cancers,[2,12–14] and cardiovascular disorders.[15,16] The involvement of aberrant and/or overexpressed Src tyrosine kinase in osteoporosis and several proliferative diseases, have made the development of inhibitors that block Src kinase desirable as potential therapeutic agents.[17,18]

SFKs share common structural motifs that determine their cellular and catalytic activity. The homologous domains include: 1) the fatty acid acylation domain, which targets the kinases to the plasma membrane, 2) the Src homology 3 (SH3) and Src homology 2 (SH2) domains, 3) the kinase domain (catalytic, including ATP and substrate binding sites), and 4) the C-terminal regulatory domain.[19,20] The conserved catalytic domain (~260-amino acid) folds into two structurally dissimilar lobes, that is, the N- and C-terminal lobes that are associated with ATP binding and peptide/protein binding, respectively.[21] These lobes are joined by a linker peptide coil of five to six residues, called the hinge region. ATP itself, and most ATP binding site inhibitors,[17,18] bind to kinases in a similar manner through a tridentate hydrogen bonding motif linked to the backbone of the hinge region. A significant body of data on nucleotide analogues has suggested that the principal course of affinity of nucleotides for kinases comes from the adenine group rather than the ribo-phosphate moieties.[22–24] X-ray studies of a number of phenylpyrazolopyrimidine derivatives,[19,25] with Hck and Lck kinases, respectively, have revealed a deep, hydrophobic binding pocket near the ATP binding site for the aryl moiety of the pyrazolopyrimidine template.

A number of kinase-domain inhibitors have been designed to inhibit the binding of ATP (ATP binding site inhibitors)[26,27] or the protein substrate (substrate-binding site inhibitors).[28–32]

[a] *Prof. K. Parang*
*Department of Biomedical and Pharmaceutical Sciences, College of Pharmacy, University of Rhode Island*
*41 Lower College Road, Kingston, Rhode Island, 02881 (USA)*
*Fax: (+1) 401-874-5787*
*E-mail: kparang@uri.edu*

[b] *Dr. A. Kumar*
*Department of Biomedical and Pharmaceutical Sciences, College of Pharmacy, University of Rhode Island*
*41 Lower College Road, Kingston, Rhode Island, 02881 (USA) and Chemistry Group, Birla Institute of Technology and Science, Pilani, Rajasthan, India 333031*

[c] *Dr. Y. Wang, Dr. X. Lin, Prof. G. Sun*
*Department of Cell and Molecular Biology*
*University of Rhode Island*
*41 Lower College Road, Kingston, Rhode Island, 02881 (USA)*

Supporting information for this article is available on the WWW under http://www.chemmedchem.org or from the author.

Several experimental inhibitors,[17,33,34] such as PP1, PP2, CGP76030, SKI606, PD173955, PD180970, and SU6656, have been used for targeting the Src family of kinases. Bicyclic *N*-heteroaromatics such as pyrazolopyrimidine and pyrrolopyrimidine have been described as potent inhibitors of c-Src and other PTKs.[27,35–37] Unfortunately, attempts to improve the biological profile of these compounds have so far met with little success. New mechanistic designed inhibitors with more structural diversity are needed to improve the potency of these compounds against Src kinase.

A number of 3-phenylpyrazolpyrimidine (PhPP) derivatives, such as N1-substituted carboxylic acid derivatives (**1**–**6**, Figure 1), were weak inhibitors of polyE$_4$Y phosphorylation with IC$_{50}$ values in the range of 71 to $>200$ μM.

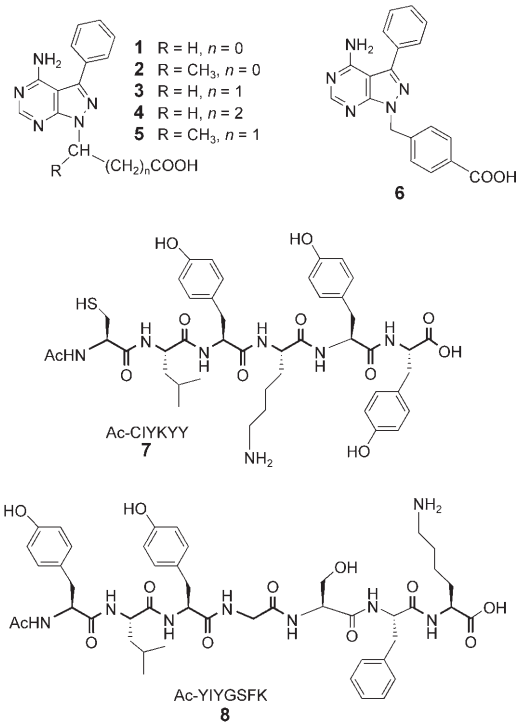


**Figure 1.** The chemical structures of selected parent analogues (**1**–**8**) for synthesizing the PhPP–peptide conjugates.

Peptides as molecular recognition motifs provide unique interactions with the kinase domain or other potential sites by appropriate orientation as they bind to domains at the kinase site that are less conserved than the ATP binding site. There has been a consistent effort to develop inhibitors that disrupt protein-substrate binding. These efforts identified preferred peptide substrates for a number of PTKs, but the affinity between the peptides and the PTKs were weak. One of the best examples from these studies is YIYGSFK[30,38] ($K_m = 55$ μM) which was reported to be a peptide substrate for c-Src and an inhibitor of Src. The peptide CIYKYY was reported to be a potent inhibitor of Src phosphorylation of YIYGSFK at 55 μM in a kinase assay.[29,30] We showed that the c-Src inhibition by YIYGSFK and CIYKYY depends on the substrate used in the kinase assay. PolyE$_4$Y is a nonspecific substrate that has multiple tyrosine residues that are phosphorylated by all eukaryotic protein tyrosine kinases. Our radioactive kinase assay showed that both Ac-CIYKYY (**7**, IC$_{50}$ = 400 μM) and Ac-YIYGSFK (**8**, IC$_{50}$ = 570 μM) (Figure 1) were weak inhibitors of polyE$_4$Y phosphorylation[39] by active c-Src.

Within our efforts to develop more potent Src-kinase inhibitors, we investigated whether the PhPP–peptide conjugates (**9**, Figure 2) of parent weak inhibitors (**1**–**8**) can generate the synergistic inhibition effect against active c-Src. Different approaches have been previously examined for the possibility of using bisubstrate analogue inhibitors against protein kinases.[22,40,41] Some of the bisubstrate approaches target the ATP binding site in combination with another specific site such as the substrate binding site[40] or the SH2 domain.[41] Negatively charged ATP, a common substrate for several enzymes, was used as the ATP binding site inhibitor in these strategies. For example, we previously synthesized a potent and selective peptide-ATP bivalent inhibitor that binds to the ATP-binding site and the substrate-binding site of the insulin receptor kinase (IRK). The X-ray crystallographic structure confirmed that the nucleotide and peptide portions of the bisubstrate inhibitor were binding to the ATP and protein substrate-binding sites, respectively.[40]

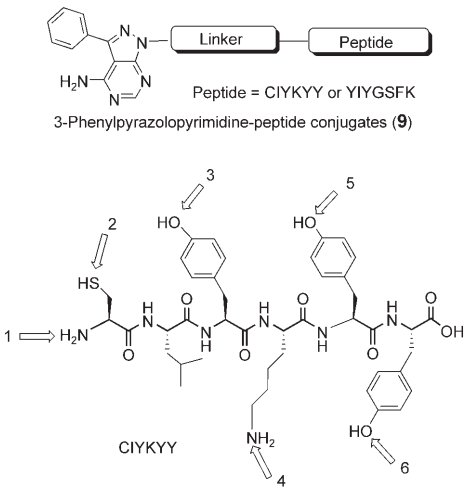


**Figure 2.** General structure of PhPP–peptide conjugates (**9**) and potential sites in CIYKYY for the attachment to a PhPP-linker.

PhPP–peptide conjugates differ from reported bisubstrate inhibitors of protein kinases that use ATP as the ATP binding motif. In these new conjugates, the ATP motif was modified to an *N*-heteroaromatic ring to avoid negatively-charged ATP. Therefore, the attachment of the peptide and pyrazolopyrimidine was not arbitrary and was based on the mechanism-based inhibition of kinases by targeting two binding sites and avoiding the negatively charged ATP by using an ATP mimic (that is, pyrazolopyrimidine). Furthermore, the previously reported bisubstrate approaches did not provide any opportunity for exploring other potential sites within the kinase domain

  

that may have important direct or indirect roles in substrate recognition or substrate binding. In the case of the ATP–peptide conjugates, peptides were connected to the γ-phosphate of ATP.[40] By the attachment of the peptide to ATP, the peptide moiety is oriented directly toward the substrate binding site by the ribo-phosphate. The attachment of peptide to γ-phosphate of ATP blocks potential interactions of the peptide with other unexplored potential binding sites within the kinase domain. In other words, there is a geometric boundary on the substrate alignment in the catalytic site of protein kinases and the peptide moiety does not have enough conformational freedom to bind to other potential sites. In PhPP–peptide conjugates (**9**), the binding and orientation of the peptide moiety is not imposed by the presence of ribo-phosphate of ATP. The functional groups of the peptide have more freedom to find appropriate orientation for novel binding interactions within the kinase domain. PhPP was attached to the N terminus or the side chain of amino acids in the peptide template through a short linker. For example, six positions were selected for the attachment of PhPP to CIYKYY (Figure 2). Thus, the approach was rationalized based on the successful design of bivalent inhibitors targeting the kinase domain, removal of the negatively-charged ATP, and generation of novel binding interactions between the PhPP–peptide conjugate and the kinase domain by the proper orientation of the peptide.

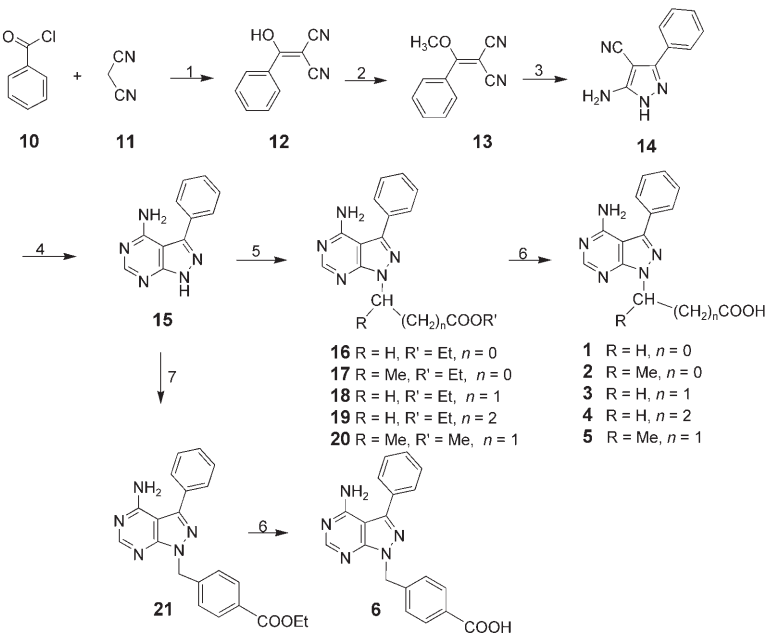


**Scheme 1.** Synthesis of N1-substituted PhPP carboxylic acid derivatives: 1) NaH, THF; 2) $(CH_3O)_2SO_2$, $NaHCO_3$; 3) $NH_2NH_2$, $NEt_3$, ethanol; 4) $HCONH_2$, reflux; 5) RCH(Br)-$(CH_2)_nCOOEt$, $K_2CO_3$, DMF; 6) NaOH; 7) $BrCH_2PhCOOEt$, $K_2CO_3$, DMF.

## Results and Discussion

### Chemistry

The synthesis of PhPP–peptide conjugates was carried out with the reaction of PhPP carboxylic acid derivatives (**1**–**6**) with appropriately protected peptides assembled on a solid-phase resin. Scheme 1 displays the synthesis of a number of PhPP carboxylic acid derivatives (**1**–**6**). The synthesis of 3-phenyl-1*H*-pyrazolo[3,4-*d*]pyrimidine-4-ylamine (**15**) was accomplished by the modification of the previously described method.[42] 2-Benzoylmalononitrile (**12**) was synthesized from the reaction of benzoyl chloride (**10**) with malononitrile (**11**) in the presence of sodium hydride in THF. Methylation of **12** with dimethyl sulfate in the presence of sodium bicarbonate in dioxane afforded 2-(methoxyphenylmethylene)malononitrile (**13**), which was cyclized by treatment with hydrazine hydrochloride in the presence of triethylamine to 5-amino-3-phenyl-1*H*-pyrazolo-4-carbonitrile (**14**). Reaction of **14** with formamide at 180 °C for 24 h afforded **15**. Compound **15** was subjected to reactions with ethyl 2-bromoacetate, ethyl 3-bromopropionate, ethyl 2-bromopropionate, ethyl 4-bromobutyrate, methyl 3-bromobutyrate, or ethyl 4-(bromomethyl)benzoate in the presence of potassium carbonate in dry *N*,*N*-dimethylformamide (DMF) to afford the corresponding ethyl ester derivatives of PhPP (**16**–**21**). Only the N1-endocyclic amino group of PhPP derivatives were reacted with bromo-substituted analogues. Unprotected N4-exocyclic amine was not reactive in this reaction condition as shown previously.[35,43] Ester hydrolysis of **16**–**21** with sodium hydroxide produced PhPP carboxylic acids (**1**–**6**). Compounds **2** and **5** were obtained as a racemic mixture.

PhPP carboxylic acid derivatives (**1**–**6**) were used for the conjugation reactions with assembled peptides on the solid-phase resin to synthesize PhPP–peptide conjugates. These compounds included N-terminal substituted (**22**–**42**) (Figure 3) and side-chain substituted (**52**–**57**) peptide derivatives of PhPP (Figure 4). Most of the synthesized compounds were based on peptide sequences CIYKYY and YIYGSFK. To investigate whether the sequences of CIYKYY and YIYGSFK are important for appropriate interactions with the kinase domain and generating synergistic inhibitory potency, other control peptides, such as EEIYGEFF, EIYGEFKK, IYGEFKKK, and AEEEIYGEFEAKKKK, were also conjugated to PhPP resulting in compounds **39**–**42**, used for comparative studies.

All final compounds were purified using preparative HPLC and characterized by a high-resolution time-of-flight mass spectrometer.

The peptides were assembled on solid phase (Wang resin) using *N*-(9-*f*luorenyl)methoxycarbonyl (Fmoc)-based chemistry and Fmoc-protected amino acids or resins (Fmoc-Tyr(*t*Bu)-Wang resin ($Y^6$), Fmoc-Tyr(*t*Bu)-OH ($Y^5$), Fmoc-Lys(Boc)-OH ($K^4$), Fmoc-Tyr(*t*Bu)-OH ($Y^3$), Fmoc-Ile-OH ($I^2$), and Fmoc-Cys(Trt)-OH ($C^1$) for CIYKYY and Fmoc-Lys(Boc)-Wang resin ($K^7$), Fmoc-Phe-OH ($F^6$), Fmoc-Ser(*t*Bu)-OH ($S^5$), Fmoc-Gly-OH ($G^4$), Fmoc-Tyr-(*t*Bu)-OH ($Y^3$), Fmoc-Ile-OH ($I^2$), and Fmoc-Tyr(*t*Bu)-OH ($Y^1$) for YIYGSFK. 2-(1*H*-Benzotriazole-1-yl)-1,1,3,3-tetramethyluronium hexafluorophosphate (HBTU) and *N*-methylmorpholine (NMM) in DMF were used as coupling and activating reagents, respectively.[39,44,45] As representative examples, the synthesis of

  

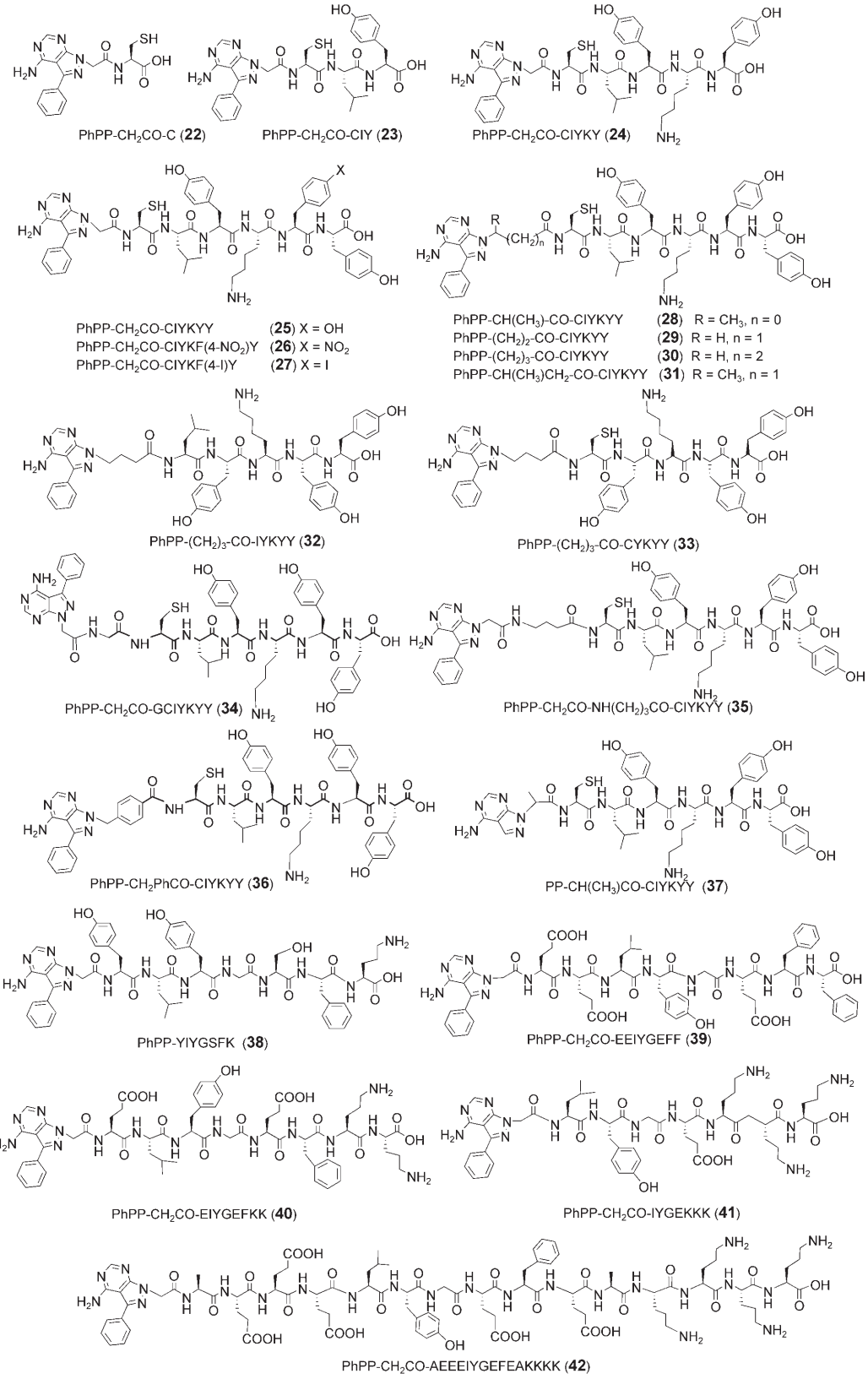


**Figure 3.** Chemical structures of N-terminal substituted peptide derivatives of PhPP (**22**–**42**).

PhPP–peptide conjugates **25**, **28**–**31**, and **34**–**36** is shown in Scheme 2. The resin-linked peptides (**44**, **50**, and **51**) were reacted with PhPP substituted with alkyl- or arylcarboxylic acids in the presence of HBTU and *N*,*N*-diisopropylethylamine (DIPEA). The compounds were deprotected and cleaved from solid support in the presence of TFA/water/anisole/ethanedi-

  

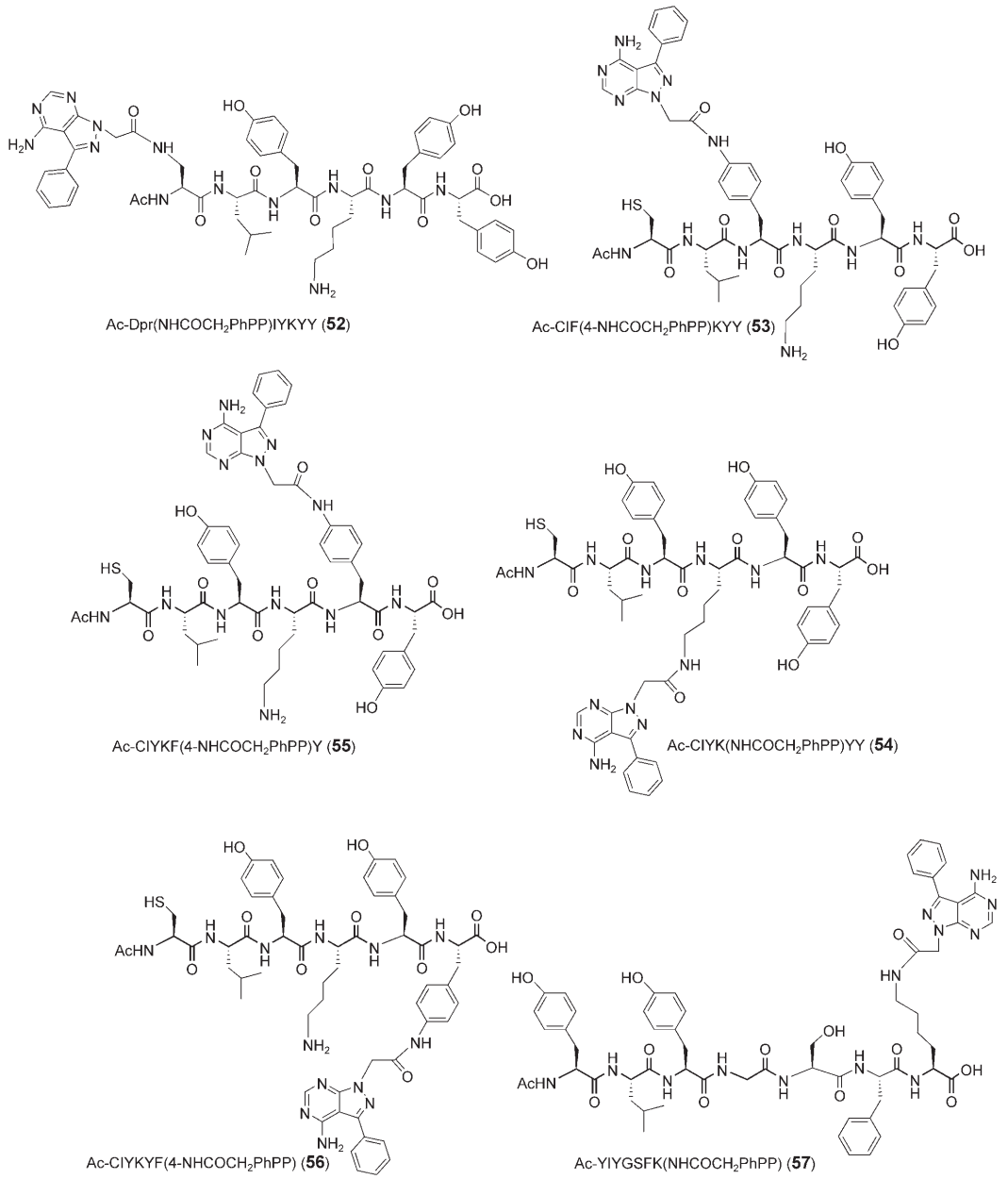


**Figure 4.** Chemical structures of side-chain PhPP-substituted peptides (**52**–**57**).

thiol (EDT) to afford N-terminal substituted PhPP–peptide conjugates **25**, **28**–**31**, and **34**–**36**.

In addition to N-terminal substituted analogues, PhPP-$CH_2COOH$ (**1**) was attached to the side chain of different amino acids in the peptides (see **52**–**57**, Figure 4). The peptides were assembled on a solid-phase resin using appropriately protected amino acids, such as Fmoc-Phe(4-$NO_2$)-OH, Fmoc-Lys(Dde)-OH, and Fmoc-Dpr(ivDde)-OH replacing tyrosine, lysine, or cysteine residues, respectively, and were N-terminally acetylated with acetic anhydride. The peptides containing a 4-nitrophenylalanine residue underwent a reduction reaction with stannous chloride under acidic conditions to yield the corresponding peptides containing 4-aminophenylalanine. The ivDde- and Dde-protecting groups in the peptides containing diaminopropionic acid (Dpr) and lysine residues, respectively, were selectively removed with 2% hydrazine monohydrate in DMF. The resin-linked peptides were subjected to reaction with PhPP-$CH_2COOH$ (**1**) in the presence of HBTU and DIPEA. The deprotection and cleavage of the compounds from the resin with TFA:anisole:water:EDT and HPLC purification afforded PhPP–peptide conjugates (**52**–**56**) (Scheme 3). A similar procedure was used for the synthesis of **57**.

### Structure–activity relationships

A number of PhPP derivatives have been described as potent inhibitors of SFKs.[19,25,36] The pyrazolopyrimidine core resembles the purine core of ATP itself and binds in the nucleotide

  

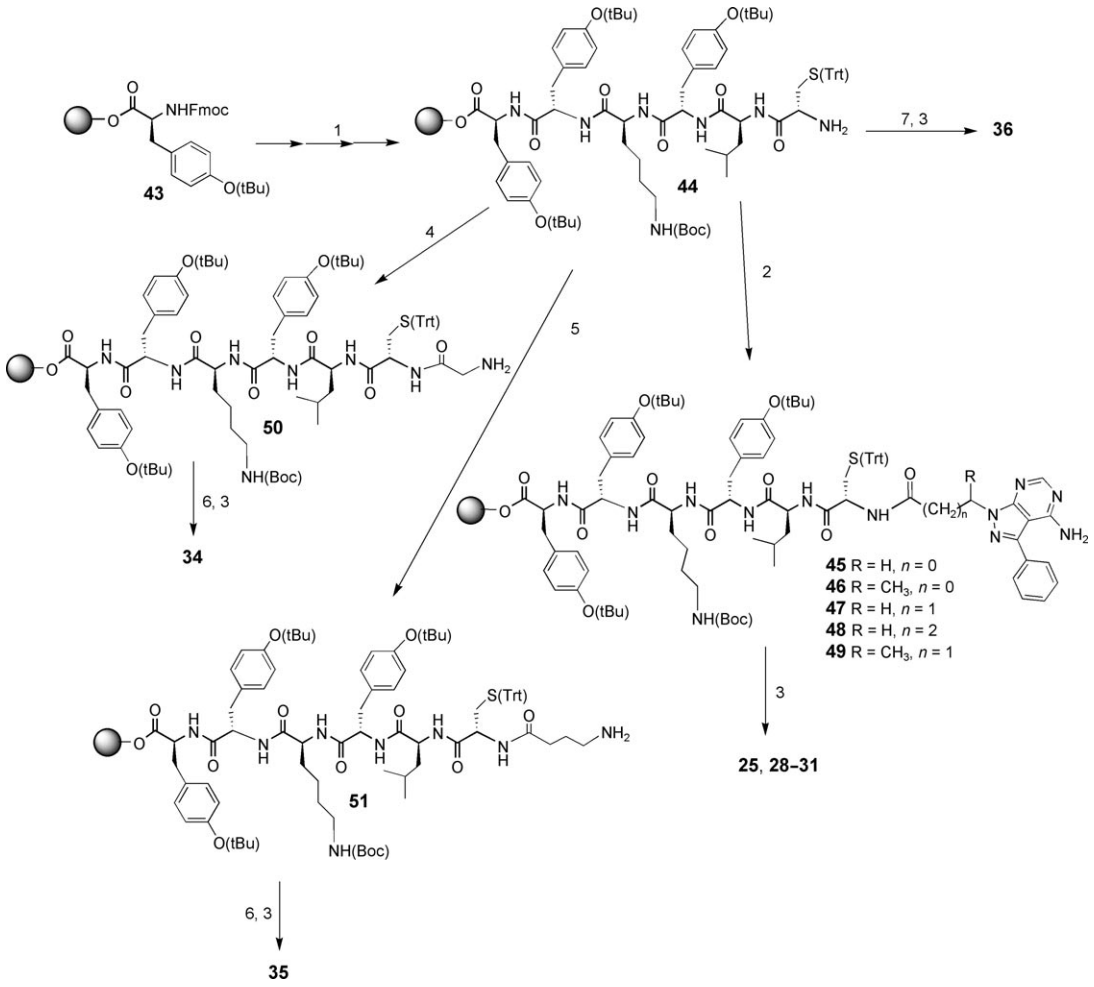


**Scheme 2.** Synthesis of N-terminal substituted peptide derivatives of PhPP (**25**, **28**–**31**, **34**–**36**): 1) Fmoc solid-phase synthesis; 2) **1**–**5**, HBTU, DIPEA, DMF; 3) TFA/water/anisole/EDT (95:2.0:2.0:1.0 *v/v/v/v*); 4a) Fmoc-Gly-OH, HBTU, b) Piperidine; 5a) FmocNH$(CH_2)_3$COOH, HBTU, b) Piperidine; 6) **1**, HBTU, DIPEA, DMF; 7) **6**, HBTU, DIPEA, DMF.

binding site in the position normally occupied by the adenine base (Figure 5) to both down- and upregulated forms of the enzyme.[19,25]

Kinase recognition of protein substrates does not depend exclusively on the phosphorylation site sequences. There are several other sites that can be explored for developing inhibitors against PTKs. For example, protein kinases use remote docking sites to aid substrate recognition and enhance substrate specificity.[46,47] Recently, we discovered the Csk docking site of Src.[48,49]

Several PhPP carboxylic acid derivatives (**1**–**6**) and peptides **7** and **8** were weak inhibitors of Src kinase catalytic activity. PhPP–peptide derivatives were designed and synthesized to exploit the ATP binding site molecular recognition motif in combination with other recognition motifs and to improve the inhibitory potency of peptide and PhPP derivatives against active c-Src. Several factors were considered for the attachment of the peptide to PhPP derivatives, including finding the right position for the attachment of the linker, using an appropriate linker, and attachment of the PhPP to different side chains. A series of peptide analogues were previously synthesized by functional group modifications in peptide side chains or by introducing conformational constraints.[39] Some of the identified potent peptides were used in this study (see compounds **26** and **27**). Compounds **26**, **27**, **39**–**42** had completely different peptide sequences.

To attach PhPP to peptides, it was necessary to determine the best position in the heterocyclic ring for the attachment to selected peptides. The N4-exocyclic amino group of the PhPP is hydrogen bonded to the side chain of Thr 338 and the carbonyl of Glu 339 of Src kinase. It has been previously reported that tethering bulky chemical groups to PP1 through its exocyclic amine (N4) yields weak inhibitors,[50] owing to the unfavorable interactions[51–53] with a structurally conserved amino acid residue 338 that contains a bulky side chain in all known eukaryotic protein kinases. Thus, a large substituent at the N4 position cannot be tolerated and leads to decreased activity. Consequently, the linkers were attached at the N1-position to synthesize modified PhPP derivatives (**1**–**6**). The PhPP analogues were attached to the N-terminal or the side chains of the peptides to establish structure–activity relationships.

  

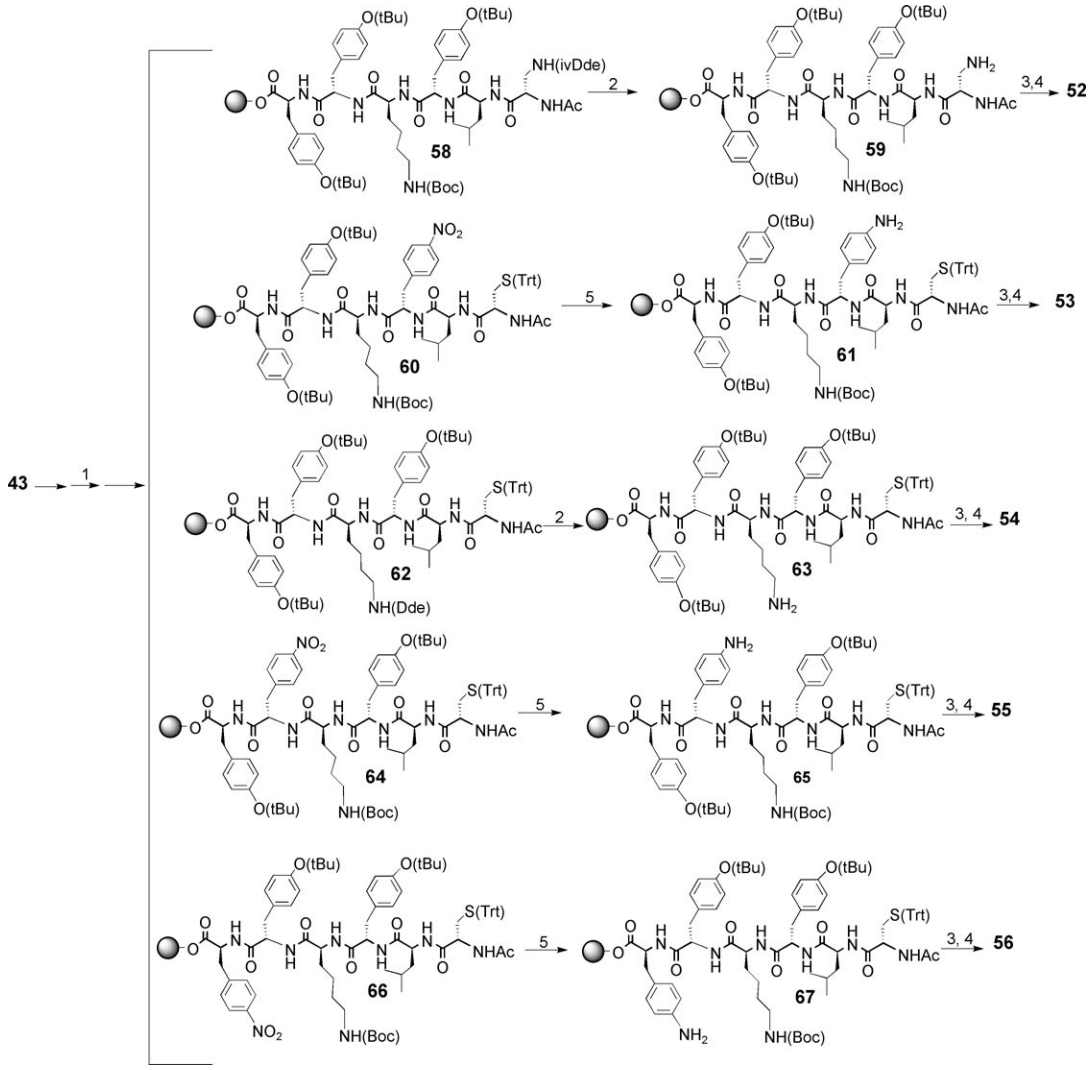


**Scheme 3.** The synthetic procedure for the preparation of PhPP-peptide conjugates **52**–**56**: 1a) Fmoc-solid-phase peptide synthesis; b) Acetic anhydride, DMF; 2) 2% Hydrazine hydrate in DMF; 3) **1**, HBTU, DIPEA, DMF; 4) TFA:anisole:water:EDT (95:2.0:2.0:1.0 *v/v/v/v*); 5) $SnCl_2 \cdot 2H_2O$/DMF.

### N1-substituted 3-phenylpyrazolopyrimidine derivatives

Any substituent attached to N1 of pyrazole occupies a mostly hydrophobic cavity that is normally occupied by ribophosphate (Figure 5a). Most of this hydrophobic cavity remains unfilled and could theoretically accommodate additional structural elements attached to PhPP. This cavity, in part, formed from side chains of helix αC and helix αD and is largely unexplored for designing inhibitors of Src kinase. The inhibitory potencies of N1-substituted PhPP-linkers (**1**–**6**) were evaluated (Table 1). PhPP-$CH_2$COOH, a PhPP derivative substituted with -$CH_2$COOH at the N1-endocyclic amine, exhibited weak inhibitory potency ($IC_{50}$ = 250 μM). A similar pattern was observed by the attachment of alkyl carboxylic acids containing other alkyl chains (**2**–**4**) or attachment of aryl carboxylic acid (**6**). Molecular modeling studies indicated that the carboxylic acids in compounds **1**–**6** have possibly unfavorable electrostatic interactions with the carboxylic acid side chain of Asp 386 (Figure 5b). This residue is in the proximity of the cavity occupied by the ATP binding site inhibitors. When the methyl group was incorporated on the β-carbon of the side chain of alkyl carboxylic acid, a slightly higher inhibitory potency ($IC_{50}$ = 71 μM) was observed (**5** versus **3**); this may be due to the enhanced hydrophobic interaction by the methyl group with the hydrophobic cavity. Ethyl ester derivatives **16** and **20** improved the inhibitory potency slightly when compared to the corresponding carboxylic acid derivatives **1** and **5**, respectively, confirming that the short carboxylic acids at N1 substituents have unfavorable electrostatic interactions.

As it was possible to improve the inhibitory potency in N1-substituted analogues by structure modifications and because of the presence of an unfilled hydrophobic cavity in proximity of N1 of PhPP, this position was selected for the attachment of peptide analogues. PhPP derivatives lack the carbohydrate and triphosphate groups (ribo-phosphate) present in the ATP. Thus, the peptides in PhPP–peptide conjugates may have the freedom to bind and to interact with potential binding sites if they are orientated properly. The 3-phenyl group occupies another

  

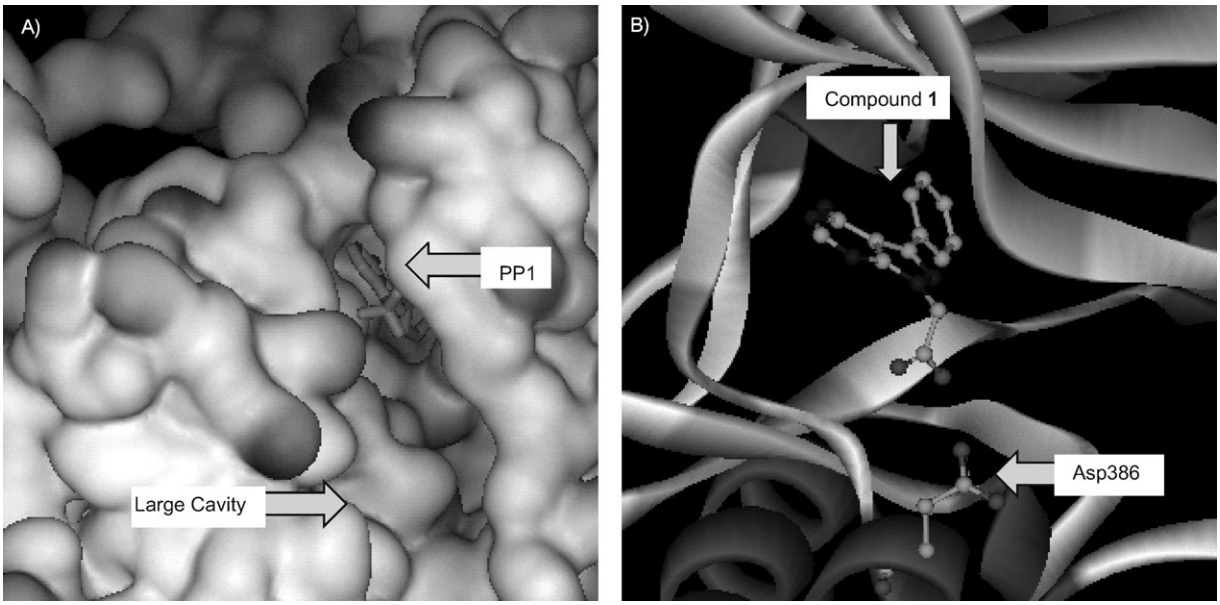


**Figure 5.** Simulated binding of a) PP1 and b) compound **1** to c-Src based on the crystal structures of PP1–Hck complex (1QCF)[19] and the AMP–PNP complex with c-Src (2SRC).[54]

**Table 1.** Chemical Structures and Inhibitory Potency Values ($IC_{50}$) for N1-Substituted 3-Phenylpyrazolo[3,4-*d*]pyrimidine Derivatives.

| Compd. | R | $IC_{50}$ [μM][a] |
|---|---|---|
| **1** | -$CH_2$COOH | 250 |
| **2** | -CH($CH_3$)COOH | >200 |
| **3** | -$CH_2CH_2$COOH | 220 |
| **4** | -$CH_2CH_2CH_2$COOH | 293 |
| **5** | -CH($CH_3$)$CH_2$COOH | 71 |
| **6** | -$CH_2$-Ph-COOH | >220 |
| **16** | -$CH_2$COOEt | 160 |
| **20** | -CH($CH_3$)$CH_2$COOEt | 12 |

[a] $IC_{50}$ is the concentration required to produce 50% inhibition in the phosphorylation of poly$E_4$Y by active c-Src (average of triplicate experiments). The upper limit of the standard error of the mean (SEM) was ±5%.

hydrophobic cavity and distances itself from any substitution on the N1 position.

### Attachment of PhPP to N-terminal position of peptides through short linkers

We investigated whether the attachment of specific Src peptide inhibitors to the N1-endocyclic amine of PhPP, through a short linker, can improve the inhibitory potency and/or generate synergistic inhibition effect when compared to parent PhPP and peptide analogues. N-terminal PhPP-substituted peptides (**22**–**42**) were synthesized (Figure 3) using PhPP as the ATP mimic and CIYKYY[29] and YIYGSFK[30] as peptide substrates.

Table 2 shows the chemical structures and inhibitory potency values for N1-substituted PhPP–peptide conjugates. Among all N-terminal PhPP-substituted peptides, compounds **25** ($IC_{50}$ = 0.38 μM) and **38** ($IC_{50}$ = 2.7 μM) inhibited the poly$E_4$Y phosphorylation by active Src significantly higher than that of parent PhPP analogue (**1**, $IC_{50}$ = 250 μM) and peptides, Ac-CIYKYY (**7**, $IC_{50}$ = 400 μM) and Ac-YIYGSFK (**8**, $IC_{50}$ = 570 μM), respectively. The compounds had significantly higher inhibitory

**Table 2.** Chemical Structures and Inhibitory Potency Values ($IC_{50}$) for N1-Substituted PhPP–peptide conjugates-

| Compd. | R | $IC_{50}$ [μM][a] |
|---|---|---|
| **7** | Ac-CIYKYY | 400 |
| **8** | Ac-YIYGSFK | 570 |
| **22** | PhPP-$CH_2$CO-C | 750 |
| **23** | PhPP-$CH_2$CO-CIY | 55 |
| **24** | PhPP-$CH_2$CO-CIYKY | 0.70 |
| **25** | PhPP-$CH_2$CO-CIYKYY | 0.38 |
| **26** | PhPP-$CH_2$CO-CIYKF(4-$NO_2$)Y | 0.90 |
| **27** | PhPP-$CH_2$CO-CIYKF(4-I)Y | 0.54 |
| **28** | PhPP-CH($CH_3$)-CO-CIYKYY | 18 |
| **29** | PhPP-($CH_2$)$_2$-CO-CIYKYY | 16 |
| **30** | PhPP-($CH_2$)$_3$-CO-CIYKYY | 4.7 |
| **31** | PhPP-CH($CH_3$)$CH_2$-CO-CIYKYY | 112 |
| **32** | PhPP-($CH_2$)$_3$-CO-IYKYY | 57 |
| **33** | PhPP-($CH_2$)$_3$-CO-CYKYY | 18.6 |
| **34** | PhPP-$CH_2$CO-GCIYKYY | 8 |
| **35** | PhPP-$CH_2$CO-NH($CH_2$)$_3$CO-CIYKYY | 1.1 |
| **36** | PhPP-$CH_2$PhCO-CIYKYY | 0.80 |
| **37** | PP-CH($CH_3$)CO-CIYKYY | 1000 |
| **38** | PhPP-YIYGSFK | 2.7 |
| **39** | PhPP-$CH_2$CO-EEIYGEFF | 63[b] |
| **40** | PhPP-$CH_2$CO-EIYGEFKK | >100[b] |
| **41** | PhPP-$CH_2$CO-IYGEKKK | >100[b] |
| **42** | PhPP-$CH_2$CO-AEEEIYGEFEAKKKK | 25[c] |

[a] $IC_{50}$ is the concentration required to produce 50% inhibition in the phosphorylation of poly$E_4$Y by active c-Src (average of triplicate experiments). The upper limit of the standard error of the mean (SEM) was ±5%; [b] Ac-EEIYGEFF, Ac-EIYGEFKK, and Ac-IYGEKKK showed an $IC_{50}$ value of >100 μM; [c] $IC_{50}$ value for peptide Ac-AEEEIYGEFEAKKKK was 74 μM.

  

potency than 3-phenylpyrazolpyrimdine (PhPP) parent derivatives, such as N1-substituted carboxylic acid derivatives (**1**–**6**, Figure 1) that had $IC_{50}$ values in the range of 71 to $>200$ μM. These data suggest a synergistic inhibition effect of the conjugation of the ATP mimic with the peptide by possibly creating favorable interactions between the conjugate and the kinase domain. The geometric and electronic features in the peptides may have contributed to binding of such compounds to c-Src kinase.

A molecular modeling study was performed where the most potent inhibitor **25** was docked in the Src kinase domain (Figure 6). It has to be emphasized that considering the high flexibility of the docked molecule, multiple binding modes could take place. The predicted binding mode was based on the minimization method described in the experimental section. Further structural studies are needed to confirm the binding modes of these compounds. The modeling studies were used to provide insights about the mode of the binding of the analogues and to determine whether the binding correlates with inhibitory potencies for potent and weak inhibitors. CIYKYY has a number of functional groups in the side chain of the amino acids, such as thiol, isopropyl, phenolic, and amino groups of cysteine, isoleucine, tyrosine, and lysine residues. Based on the simulated molecular modeling, CIYKYY in PhPP–peptide conjugate **25** occupies the large cavity that is normally unoccupied by ATP binding site inhibitors. Molecular modeling studies showed the formation of two favorable hydrogen bonds for tyrosine $Y^6$. The hydrogen bonds were formed between the oxygen in the carbonyl (C*O*OH) of the carboxylic acid terminal in tyrosine $Y^6$ with the side chain of Arg 388 (N*H*$_2$) (distance $\approx$2.1 Å) and the O*H* of the carboxylic acid terminal (COO*H*) in tyrosine $Y^6$ with the carbonyl in the side chain carbonyl group of Gln 277 (C*O*NH$_2$) (distance $\approx$2.1 Å). Furthermore, Tyr 416 (O*H*) exhibited hydrogen bonding with the carbonyl amide oxygen (C*O*NH) of $Y_5$ in **25** (distance $\approx$2.1 Å). Phosphorylation of Tyr 416 (autophosphorylation) located in the activation loop blocks the inactivation of Src kinases by C-terminal phosphorylation.[20] It remains to be determined whether the predicted hydrogen bonds of $Y^5$ with Tyr 416 (*OH*) has any direct effect on autophosphorylation of Tyr 416 and Src kinase activity. The lysine side chain (*N*H$_2$, $K^4$) and the tyrosine side chain of (O*H*, $Y^5$) of compound **25** form hydrogen bonds with the side chain N*H*$_2$ of Lys 295 (distance $\approx$1.8 Å) and the aromatic amino group of His 384 (ND$_1$) (distance $\approx$2.1 Å), respectively. The 3-phenyl group of PhPP is oriented towards the hydrophobic pocket in the back of the binding site as expected, but the mode of bonding of PhPP in the ATP binding site of Src was different from PP1 for binding to Hck.[19] The phenyl group in **25** does not penetrate very deeply into the hydrophobic pocket (Figure 6). The amino group (N4) of the PhPP is hydrogen bonded to the N*H* of the amide group in Lys 343 (distance $\approx$2.0 Å) (Figure 6). Therefore, the attachment of CIYKYY to PhPP generated novel geometric and electronic features that contributed to binding of **25** to c-Src kinase. The interactions of the functional groups with several amino acids in the kinase domain, such as those in the hinge region, the substrate binding site, and the activation domain, may have contributed to the enhancement of potency.

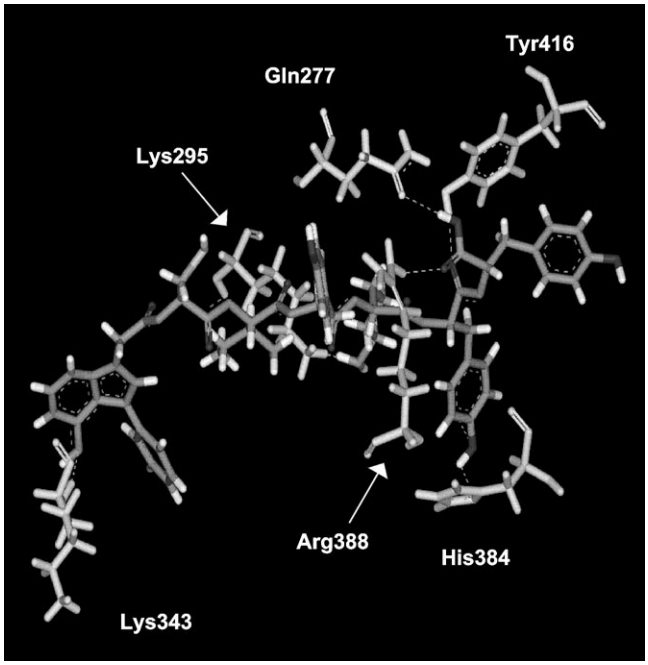


**Figure 6.** Predicted major interactions of compound **25** with amino acids of the Src kinase domain. Compound **25** and side chains of amino acids of the Src kinase domain are represented by sticks. Hydrogen atoms have been removed to improve clarity. The key amino acids residues within the Src kinase domain are labeled. The binding pocket amino acids form hydrogen bonds with different functional groups of the PhPP–peptide conjugate. The figure were drawn using the Accelrys visualization system.

### Deletion of amino acids

The presence of the specific amino acids seems to be critical for generating the inhibitory potency. The removal of amino acids in the peptide chains of CIYKYY in the PhPP–peptide conjugates reduced the inhibitory potency possibly by eliminating or reducing potential interactions of the peptide with the kinase domain. For example, compound **22** lacked IYKYY and exhibited a reduced inhibitory potency of approximately 2000-fold when compared to **25** (Table 2). The PhPP–peptide conjugate **23** that did not have KYY, had reduced inhibitory activity of approximately 145-fold when compared to **25**. Approximately half of the inhibition activity was lost in **24** when the C-terminal tyrosine was removed in the conjugate **25**. The results indicate that $K^4$, $Y^5$, and $Y^6$ are required for generating the maximum inhibitory activity. Molecular modeling studies suggested that removal of these amino acids will eliminate the critical hydrogen bonding interactions between the conjugate and the amino acids in the kinase domain as shown for compound **25** (Figure 6b). Minor amino acid modifications, such as using 4-nitrophenylalanine or 4-iodophenylalanine in **26** and **27** in place of $Y^5$ in **25**, did not reduce the inhibitory potency significantly.

  

### The nature and size of the linker

The nature and the length of the linker appeared to be important in the inhibitory activity. To determine the importance of the linker distance, several PhPP–peptide conjugates were prepared that had longer linkers between the peptide and PhPP. The incorporation of methyl groups in the linker diminished the inhibitor potency as seen in **28** and **31** (Table 2) compared to the corresponding compounds **25** and **29** without the methyl group. However, the conjugate **28** was more potent compared to the parent PhPP **2** ($IC_{50} > 200$ μM) containing the linker with carboxylic acid. Compound **30** with an additional methylene group in the linker had approximately 3.5-fold more inhibitory potency than **29**. Similar to that described above for **25**, the elimination of amino acids such as cysteine in **32** and isoleucine in **33** reduced the inhibitory potency when compared to that of **30**. A similar pattern for improving the inhibitory potency by lengthening of the linker was observed when comparing **34** and **35**. The incorporation of glycine between the PhPP and cysteine residue in **34** reduced the inhibitory potency by 21-fold when compared to **25**. Increasing the length of the linker by using γ-aminobutyric acid in **35** improved the inhibitory potency ($IC_{50} = 1.1$ μM). The incorporation of a phenyl group between the PhPP and the cysteine residue in **36** significantly improved the inhibitory potency ($IC_{50} = 0.8$ μM). Consequently, the nature and length of the linker appear to effect directly the orientation of the peptide and inhibitory potency. Overall, these studies underscore the importance of linker length for achieving a high affinity interaction and maximal inhibition.

### Deletion of the phenyl group

The compound **37** that lacks the 3-phenyl moiety exhibited no inhibitory potency compared to the corresponding compound containing the phenyl moiety (**28**, $IC_{50} = 18$ μM) (Table 2). The phenyl substituent in PhPP inserts into the hydrophobic pocket towards the back of the binding site (Figure 5). These results suggest that the hydrophobic interaction of the phenyl group with hydrophobic pocket is essential for the binding of PhPP to the ATP binding site. By removing the phenyl group, the peptide moiety also loses the right orientation for binding to the kinase domain.

### Using other peptides

Using other peptides known as the Src substrate-binding site inhibitors, such as EEIYGEFF,[31] IYGEFKKK,[55] EIYGEFKK,[55] and AEEEIYGEFEAKKKK[31] in **39**–**42** for attachment to PhPP did not improve the inhibitory potency when compared to those of the CIYKYY and YIYGSFK templates **25** and **38**. Ac-AEEEIYGEFEAKKKK had an inhibitory potency of 74 μM. The attachment of PhPP to this peptide in **42** improved the inhibitory potency only by threefold. These studies suggest that the sequence of the peptide is important for appropriate interactions with the kinase domain and generating synergistic inhibitory potency, and the inhibition through the peptide is sequence dependent.

### The attachment of PhPP-$CH_2$COOH to the side chains of different amino acids in the peptide

PhPP-$CH_2$COOH (**1**) was connected to the side chain of different amino acids in the peptides (Figure 4). The position of the PhPP's *N*-heteroaromatic ring relative to the peptide substrate, $C^1I^2Y^3K^4Y^5Y^6$, proved to be critical for generating maximal inhibitory potency (Table 3). When the PhPP ring was moved along the peptide and was attached to the side chains of different amino acids, the inhibition potency was reduced.

**Table 3.** Chemical Structures and Inhibitory Potency Values ($IC_{50}$) for Side-Chain PhPP-Substituted Peptides.

| PhPP-peptide conjugate sequence | $IC_{50}$ [μM][a] |
|---|---|
| Ac-Dpr(NHCOCH$_2$PhPP)IYKYY | 64 |
| Ac-CIF(4-NHCOCH$_2$PhPP)KYY | 0.59 |
| Ac-CIYK(NHCOCH$_2$PhPP)YY | 2.1 |
| Ac-CIYKF(4-NHCOCH$_2$PhPP)Y | 2.1 |
| Ac-CIYKYF(4-NHCOCH$_2$PhPP) | 18 |
| Ac-YIYGSFK(NHCOCH$_2$PhPP) | 30 |

[a] $IC_{50}$ is the concentration required to produce 50% inhibition in the phosphorylation of poly$E_4$Y by active c-Src (average of triplicate experiments). The upper limit of the standard error of the mean (SEM) was ±5%.

The attachment of PhPP to the side chain of $C^1$ or $Y^6$ diminished the inhibitory potency significantly when compared to that of **25**. The reduction of inhibition was significant in **52** ($IC_{50} = 64$ μM), in which the PhPP was attached to the side chain of the first amino acid and where the thiol group of cysteine was substituted with the amino group of Dpr, suggesting the loss of some of the binding interactions with the kinase domain observed in **25** and/or the change in the orientation of the peptide with the attachment of the heterocyclic ring at this position. Similarly, the attachment of the N-heteroaromatic to the C-terminal amino acid in **56** and **57** reduced the inhibition by the analogues significantly. Therefore, the placement of the PhPP ring at the N-terminal of the peptide as seen in **25** appears to be optimal for generating maximal inhibitory potency.

The attachment of PhPP to amino acid residues at positions 3 (**53**), 4 (**54**), and 5 (**55**) in the CIYKYY template were less deleterious in reducing inhibitory potencies against active c-Src when compared with other peptide conjugates **52** and **56** that had PhPP at positions 1 and 6. The comparison of the interactions of compounds **25** and **53** with the Src kinase domain using molecular modeling shows that the two compounds display different binding modes. Molecular modeling studies (Figure 7) showed the formation of a favorable hydrogen bonding between the carboxylic acid (COO*H*) terminal of tyrosine ($Y^6$) of **53** with the side chain of Glu 339 (COO*H*) (distance ≈1.9 Å). The lysine side chain (N*H*, $K^4$) and the tyrosine side chain of (O*H*, $Y^6$ of compound **53** showed hydrogen bonds

  

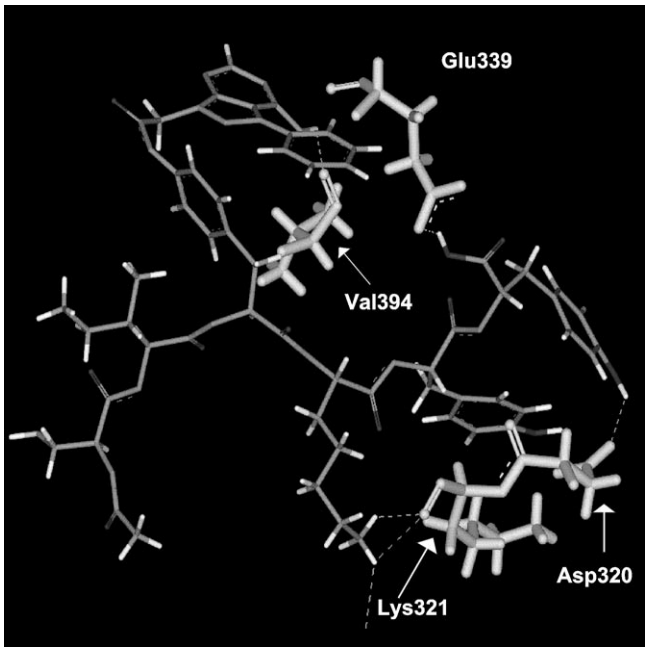


**Figure 7.** Predicted major interactions of compound **53** with amino acids of the Src kinase domain. Compound **53** and side chains of amino acids of the Src kinase domain are represented by sticks. Hydrogen atoms have been removed to improve clarity. The key amino acids residues within the Src kinase domain are labeled. The figure was drawn using the Accelrys visualization system.

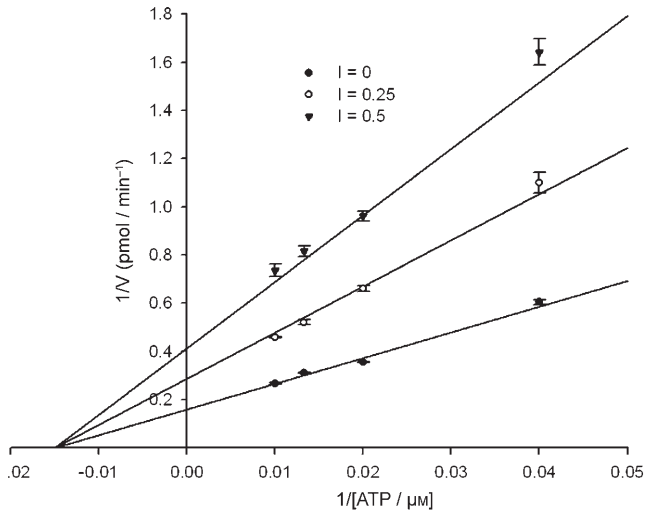


**Figure 8.** Pattern of inhibition of c-Src by compound **25**. Lineweaver–Burk plot of 1 *V* versus 1/ATP with varying concentrations of **25** shows noncompetitive inhibition ($V_m = 6.3 \pm 0.3$ pmol min$^{-1}$, $K_m = 67.0 \pm 5.5$ μM, $K_i = 0.31 \pm 0.01$ μM, $R^2 = 0.994$, AIC value = −114.6).

with the carbonyl amide oxygen (C*O*NH) of Lys 321 (distance ≈1.9 Å) and carboxylic acid (CO*O*) side chain of Asp 320 (distance ≈1.8 Å), respectively. An interesting feature is the formation of a hydrogen bond between the N*H* group of N4 in PhPP and the oxygen of carbonyl amide (C*O*NH) in Val 394 (Figure 7). This interaction stabilizes the favorable backbone conformation of **53** for other residues such as tyrosine and lysine to interact effectively with the protein, but also locks the side chain conformation of these residues with a favorable entropic contribution. The 3-phenyl group in **53** reaches fairly deep in the hydrophobic pocket.

The modeling provided insights about the mode of the binding of the analogues and was completely correlated with inhibitory potencies. Those compounds with low $IC_{50}$ values did not generate any binding interactions within the kinase domain. On the other hand, potent compounds **25** and **53** were properly oriented within the kinase domain, generating favorable hydrogen bonds between key amino acids in the peptide and the amino acids within kinase domain.

### The steady-state kinetic assay

The mechanism of inhibition by **25** was studied using variable concentrations of ATP and the inhibitor. The Lineweaver plot (Figure 8) showed that compound **25** follows a noncompetitive inhibition pattern against ATP. These results suggest that compound **25** is using other potential sites in the kinase domain for inhibiting the Src kinase activity by binding to an area of the kinase domain that does not completely overlap with the ATP binding site, such as the ATP binding site adjacent domains. These results are consistent with the previous studies of other phenylpyrazolopyrimidine derivatives. PP1 is a noncompetitive inhibitor of the ATP binding site of Src and at the same time a mixed competitive inhibitor of Poly$E_4$Y.[56] We assume that **25** like PP1 interferes with the binding of the substrate to the substrate-binding site. As shown, the 3-phenyl group in **25** does not penetrate very deeply into the hydrophobic pocket (Figure 6). The hydrophobic interaction of the 3-phenyl group of PhPP with the hydrophobic pocket was slightly reduced because of the overall orientation of the peptide. Modeling studies confirmed that the major interactions of the functional groups in the peptide moiety with amino acids are within the kinase domain but outside the binding pocket that N-heteroaromatic usually bonds. In fact, the pyrazolopyrimidine ring in **25** and **53** showed only minor interactions with Lys 343 and Val 394, respectively (Figures 6 and 7). Further kinetic studies are underway to elucidate the inhibition mechanism of these compounds. X-ray crystallographic studies of PhPP–peptide conjugates with active c-Src are required to correctly determine the binding modes of the compounds and to confirm the modeling studies.

## Conclusions

In summary, a new class of potent kinase inhibitors was discovered by introducing novel bivalent scaffolds. The synthesis and evaluation of PhPP–peptide conjugates were undertaken to improve the inhibitory potency of peptide and PhPP derivatives against active c-Src and to establish structure–activity relationships of these analogues. This approach allowed for the discovery of additional potential sites in the kinase domain for inhibitor design. The structure–activity relationships were established based on a rational approach. Herein, the main objective was to introduce a novel conceptual approach for

  

mechanistically designed inhibitors by exploiting the molecular recognition motifs within the kinase domain. We predict that selectivity can be incorporated by structure optimization in future studies as we have previously shown for other bisubstrate inhibitors,[40] but these studies were beyond the scope of the objectives of this manuscript. The structure–activity relationships provided new insights for designing inhibitors against Src. Several of the PhPP–peptide conjugates exhibited significantly higher inhibitory potencies than the corresponding parent compounds, PhPP derivatives, and peptides. This study revealed a number of important features regarding designing PhPP–peptide conjugates. The positioning of the PhPP on the N-terminal of the peptide produced the maximum inhibitory effect against Src kinase. The nature of the peptide was also important in generating inhibitory activity. Eliminating the amino acids in the peptide significantly reduced inhibitory potency. Taken together, these results suggest that further exploring and optimization of the sequence diversity of functional groups of peptide side chains in several lead compounds (**25**, **36**, **38**, or **53**) as novel templates may lead to more potent Src inhibitors. Further studies are underway to generate lead compounds that also have selectivity against SFKs.

## Experimental Section

**General.** All reactions were carried out in Bio-Rad polypropylene columns by shaking and mixing using a Glass-Col small tube rotator in dry conditions or on a PS3 automated peptide synthesizer (Rainin Instrument Co., Inc.) at room temperature unless otherwise stated. In general, all peptides were synthesized by the solid-phase synthesis strategy employing Fmoc-based chemistry and Fmoc-L-amino acid building blocks. HBTU and NMM in DMF were used as coupling and activating reagents, respectively. Fmoc-amino acid Wang resins, coupling reagents, and Fmoc-amino acid building blocks were purchased from Novabiochem. Other chemicals and reagents were purchased from Sigma–Aldrich Chemical Company. Fmoc deprotection at each step was carried out using piperidine in DMF (20%). A mixture of TFA/anisole/water/EDT (95:2.0:2.0:1.0 *v/v/v/v*) was used for side-chain deprotection of amino acids and cleavage of the synthesized peptides from the resin. The crude compounds were precipitated by the addition of cold diethyl ether ($Et_2O$) and purified by HPLC (Shimadzu LC-8A preparative liquid chromatograph; Shimadzu fraction collector 10 A) on a Phenomenex Prodigy 10 μm ODS reversed-phase column. The peptides were separated by eluting the crude peptide at 4.0 mL min$^{-1}$ using a gradient of 0–100% acetonitrile (0.1% TFA) and water (0.1% TFA) over 85 min, and then they were lyophilized. The purity of the final products was confirmed by analytical HPLC on the Hitachi system with a C18 Shimadzu Premier 3 μm column (150×4.6 mm) using two different gradient systems and a flow rate of 0.5 mL min$^{-1}$. The chemical structures of compounds were confirmed by a high-resolution PE Biosystems Mariner API time-of-flight mass spectrometer. Details of procedures and spectroscopic data of the representative compounds are presented below. The percentage overall yields for the PhPP–peptide conjugates was 20–30%.

### *Synthesis of ATP analogues.*

**2-Benzoylmalonitrile (12).** Sodium hydride (3.60 g, 150.0 mmol) was suspended in dry THF (20 mL) and the mixture was cooled to 0 °C. Malononitrile (**11**, 4.70 g, 71.1 mmol) was dissolved in dry THF (25 mL) and added dropwise to the stirring sodium hydride mixture in THF over 20 min. Benzoyl chloride (**10**, 9.0 mL, 77.5 mmol) was dissolved in dry THF (15 mL) and added dropwise to the stirring malononitrile mixture over 30 min. The reaction was allowed to warm to room temperature and stirred for an additional 30 min. Then it was acidified with 1N HCl to pH 2. The mixture was extracted with ethyl acetate (3×200 mL) and dried over anhydrous sodium sulfate. The ethyl acetate was evaporated under reduced pressure and the compound was purified by silica gel column chromatography using ethyl acetate as the eluent to afford **12** as a white solid product (11.13 g, 92%). $^1$H NMR ($CDCl_3$, 400 MHz): $\delta =$ 11.82 (s, 1H, O*H*), 7.79–7.31 (m, 3H, *m*-Ph-*H*, and *p*-Ph-*H*), 6.71–6.43 ppm (m, 2H, *o*-Ph-*H*); $^{13}$C NMR ($CDCl_3$, 100 MHz): $\delta =$ 187.48, 136.52, 132.24, 129.19, 129.02, 128.45, 118.12, 54.69 ppm; HR-MS (ESI-MS) (*m/z*): $C_{10}H_6N_2O$ calcd, 170.0480; found, 170.9921 $[M+H]^+$.

**2-(Methoxyphenylmethylene)malononitrile (13).** Sodium bicarbonate (45.30 g, 0.54 mole) was added over 10 min to a solution of **12** (11.05 g, 65 mmol) in dioxane (100 mL) and water (20 mL). Dimethyl sulfate (63.0 g, 0.50 mole) was added to the reaction mixture and the solution was heated to reflux with vigorous stirring for 3 h. The reaction mixture was cooled, diluted with water (90 mL), and extracted with diethyl ether (3×200 mL). The organic layer was dried with anhydrous sodium sulfate and evaporated under reduced pressure. The residue was purified by silica gel column chromatography using dichloromethane and methanol (3:2 *v/v*) to afford **13** (9.33 g, 78%). $^1$H NMR ($CDCl_3$, 400 MHz): $\delta =$ 7.76–7.61 (m, 5H, aromatic), 3.83 ppm (s, 3H, O$CH_3$); $^{13}$C NMR ($CDCl_3$, 100 MHz): $\delta =$ 187.32, 133.63, 129.99, 129.59, 128.73, 114.53, 113.13, 67.77, 62.44 ppm; HR-MS (ESI-MS) (*m/z*): $C_{11}H_8N_2O$ calcd, 184.0637; found, 184.9866 $[M+H]^+$.

**5-Amino-3-phenyl-1*H*-pyrazolo-4-carbonitrile (14).** Triethylamine (13.61 g, 135.0 mmol) and hydrazine hydrochloride (4.73 g, 45.0 mmol) were added to a solution of **13** (8.28 g, 45.0 mmol) in ethanol (250 mL) and refluxed for 30 min. Ethanol was evaporated under reduced pressure. The solid was resuspended in water (150 mL) and extracted with ethyl acetate (3×150 mL). The organic layer was dried with anhydrous sodium sulfate and concentrated under reduced pressure. The residue was purified by silica gel column chromatography using dichloromethane/methanol (10:1 *v/v*) as eluent to yield **14** (7.86 g, 95%). $^1$H NMR ([$D_6$]DMSO, 400 MHz): $\delta =$ 12.0 (s, 1H, N*H*), 7.81–7.76 (m, 2H, *o*-Ph-*H*), 7.56–7.37 (m, 3H, *m*-Ph-*H*, and *p*-Ph-*H*), 6.42 ppm (s, 2H, N$H_2$); $^{13}$C NMR ([$D_6$]DMSO, 100 MHz): $\delta =$ 154.68, 150.02, 145.50, 132.16, 128.72, 125.67, 116.33, 69.78 ppm; HR-MS (ESI-TOF) (*m/z*): $C_{10}H_8N_4$ calcd, 184.0749; found, 184.9967 $[M+H]^+$.

**3-Phenyl-1*H*-pyrazolo[3,4-*d*]pyrimidin-4-ylamine (15).** Compound **14** (7.73 g, 42.0 mmol) was suspended in formamide (125 mL) and heated at 180 °C for 24 h. The reaction was cooled to room temperature and poured in water. The precipitate formed was filtered. The solid obtained was dissolved in hot ethanol, decolorized with charcoal, and filtered through celite. The filtrate was concentrated under reduced pressure. The residue was purified by silica gel column chromatography using dichloromethane/methanol (20:1 *v/v*) to afford **15** (6.85 g, 77%). $^1$H NMR ([$D_6$]DMSO, 400 MHz): $\delta =$ 13.62 (s, 1H, N*H*), 8.23 (s, 1H, H-6), 7.71–7.66 (m, 2H, *o*-Ph-*H*), 7.59–7.45 (m, 3H, *o*-Ph-*H*, and *m*-Ph-*H*), 6.85 ppm (br s, 2H, N$H_2$); $^{13}$C NMR ([$D_6$]DMSO, 100 MHz): $\delta =$ 158.05, 155.81, 144.43, 142.450, 133.43, 129.11, 128.51, 128.26, 96.97 ppm; HR-MS (ESI-TOF) (*m/z*): $C_{11}H_9N_5$ calcd, 211.0858; found, 212.0153 $[M+H]^+$.

**Ethyl 2-(4-amino-3-phenyl-1*H*-pyrazolo[3,4-*d*]pyrimidin-1-yl)acetate (16).** Ethyl 2-bromoacetate (167 mg, 0.11 mL, 1.0 mmol) was added to a round-bottom flask containing **15** (211.0 mg, 1.0 mmol) and anhydrous potassium carbonate (100.0 mg) in dry DMF

  

(25 mL). The reaction mixture was stirred at room temperature for 6 h under nitrogen atmosphere and then concentrated under reduced pressure. The residue was extracted with dichloromethane (3×25 mL), concentrated under reduced pressure, and purified by silica gel column chromatography using dichloromethane/methanol as eluents (2%, *v/v*) to afford **16** (270 mg, 91%). $^1$H NMR ($CDCl_3$, 400 MHz): $\delta$ = 8.35 (s, 1H, H-6), 7.70–7.68 (m, 2H, *o*-Ph-*H*), 7.59–7.51 (m, 3H, *m*-Ph-*H*, and *p*-Ph-*H*), 5.25 (s, 2H, $CH_2$), 4.21 (quartet, $J$ = 6.8 Hz, 2H, $CH_2$), 1.25 ppm (t, $J$ = 6.8 Hz, 3H, $CH_3$); $^{13}$C NMR ($CDCl_3$, 100 MHz): $\delta$ = 167.84, 158.20, 156.06, 155.00, 144.41, 132.61, 129.21, 128.81, 128.19, 97.28, 61.28, 47.92, 14.04 ppm; HR-MS (ESI-TOF) (*m/z*): $C_{15}H_{15}N_5O_2$ calcd, 297.1226; found, 298.1276 $[M+H]^+$.

**(±) Ethyl 2-(4-amino-3-phenyl-1*H*-pyrazolo[3,4-*d*]pyrimidin-1-yl)-propanoate (17).** Compound **17** (286 mg, 92%) was synthesized from DL-ethyl 2-bromopropionate (181 mg, 0.13 mL, 1.0 mmol) and **15** (211.0 mg, 1.0 mmol) using the same procedure described above for the synthesis of **16**. $^1$H NMR ([D$_6$]DMSO, 400 MHz): $\delta$ = 8.46 (s, 1H, H-6), 7.73–7.67 (m, 2H, *o*-Ph-*H*), 7.57–7.39 (m, 3H, *m*-Ph-*H*, and *p*-Ph-*H*), 5.66 (quartet, $J$ = 7.2 Hz, 1H, C*H*), 4.12 (quartet, $J$ = 7.0 Hz, 2H, $CH_2$), 1.77 (d, $J$ = 7.2 Hz, 1H, $CH_3$), 1.12 ppm (t, $J$ = 7.0 Hz, 1H, $CH_3$); $^{13}$C NMR ([D$_6$]DMSO, 100 MHz): $\delta$ = 170.72, 159.02, 156.61, 155.45, 144.96, 133.59, 130.14, 129.89, 129.64, 129.22, 128.92, 98.27, 62.06, 55.04, 16.95, 14.83 ppm; HR-MS (ESI-TOF) (*m/z*): $C_{16}H_{17}N_5O_2$ calcd, 311.1382; found, 312.2945 $[M+H]^+$, 334.2600 $[M+Na]^+$, 350.2163 $[M+K]^+$.

**Ethyl 3-(4-amino-3-phenyl-1*H*-pyrazolo[3,4-*d*]pyrimidin-1-yl)propanoate (18).** Compound **18** (255 mg, 82%) was synthesized from ethyl 3-bromopropionate (181 mg, 0.13 mL, 1.0 mmol) and **15** (211.0 mg, 1.0 mmol) using the same procedure described above for the synthesis of **16**. $^1$H NMR ([D$_6$]DMSO, 400 MHz): $\delta$ = 8.48 (s, 1H, H-6), 7.70–7.62 (m, 2H, *o*-Ph-*H*), 7.58–7.38 (m, 3H, *m*-Ph-*H*, and *p*-Ph-*H*), 5.57 (t, $J$ = 7.0 Hz, 2H, $CH_2$), 4.16 (quartet, $J$ = 6.9 Hz, 2H, $CH_2$), 2.27 (t, $J$ = 7.0 Hz, 2H, $CH_2$), 1.16 ppm (t, $J$ = 6.9 Hz, 3H, $CH_3$); $^{13}$C NMR ([D$_6$]DMSO, 100 MHz): $\delta$ = 169.83, 159.13, 155.98, 154.74, 144.67, 133.03, 129.85, 129.76, 129.58, 129.02, 128.93, 97.96, 61.76, 54.95, 30.45, 14.78 ppm; HR-MS (ESI-TOF) (*m/z*): $C_{16}H_{17}N_5O_2$ calcd, 311.1382; found, 312.3001 $[M+H]^+$, 334.2600$[M+Na]^+$, 350.2115 $[M+K]^+$.

**Ethyl 4-(4-amino-3-phenyl-1*H*-pyrazolo[3,4-*d*]pyrimidin-1-yl)butanoate (19).** Compound **19** (243 mg, 75%) was synthesized from ethyl 4-bromobutyrate (195 mg, 0.14 mL, 1.0 mmol) and **15** (211.0 mg, 1.0 mmol) using the same procedure described above for the synthesis of **16**. $^1$H NMR ([D$_6$]DMSO, 400 MHz): $\delta$ = 8.26 (s, 1H, H-6), 7.68–7.67 (m, 2H, *o*-Ph-*H*), 7.54–748 (m, 3H, *m*-Ph-*H*, and *p*-Ph-*H*), 4.36–4.50 (br s, 2H, -N$CH_2$), 3.98 (quartet, $J$ = 6.70, 2H, $CH_2$), 2.32–2.31 (m, 2H), 2.11–2.08 (m, 2H), 1.12 ppm (t, $J$ = 6.70, 3H, $CH_3$); $^{13}$C NMR ([D$_6$]DMSO, 100 MHz): $\delta$ = 172.15, 158.16, 155.71, 154.31, 143.65, 132.97, 129.24, 129.01, 128.71, 128.35, 128.11, 97.27, 59.85, 45.52, 30.68, 24.46, 14.07 ppm; HR-MS (ESI-TOF) (*m/z*): $C_{17}H_{19}N_5O_2$ calcd, 325.1539; found, 326.3042 $[M+H]^+$, 348.2650 $[M+Na]^+$.

**(±) Methyl 3-(4-amino-3-phenyl-1*H*-pyrazolo[3,4-*d*]pyrimidin-1-yl)butanoate (20).** Compound **20** (230 mg, 74%) was synthesized from DL-methyl 3-bromobutyrate (181 mg, 1.0 mmol) and **15** (211.0 mg, 1.0 mmol) using the same procedure described above for the synthesis of **16**. $^1$H NMR ([D$_6$]DMSO, 400 MHz): $\delta$ = 8.26 (s, 1H, H-6), 7.66–7.64 (m, 2H, *o*-Ph-*H*), 7.57–7.46 (m, 3H, *m*-Ph-*H*, and *p*-Ph-*H*), 5.24–5.34 (quartet, 1H, -NC*H*), 3.51 (s, 3H, O$CH_3$), 2.43–2.56 (m, 2H, $CH_2$CO), 1.00 ppm (d, $J$ = 7.1 Hz, 3H, CH$CH_3$); $^{13}$C NMR ([D$_6$]DMSO, 100 MHz): $\delta$ = 170.01, 158.13, 155.68, 155.60, 141.20, 133.00, 129.15, 128.64, 128.25, 128.01, 97.02, 51.47, 49.16, 20.25 ppm; HR-MS (ESI-TOF) (*m/z*): $C_{16}H_{17}N_5O_2$ calcd, 311.1382; found, 312.2999 $[M+H]^+$, 334.2609 $[M+Na]^+$.

**Ethyl 4-((4-amino-3-phenyl-1*H*-pyrazolo[3,4-*d*]pyrimidin-1-yl)methyl)benzoate (21).** Compound **21** (350 mg, 94%) was synthesized from ethyl 4-(bromomethyl)benzoate (243 mg, 1.0 mmol) and **15** (211.0 mg, 1.0 mmol) using the same procedure described above for the synthesis of **16**. $^1$H NMR ([D$_6$]DMSO, 400 MHz): $\delta$ = 8.29 (s, 1H, H-6), 7.91 (d, $J$ = 7.1 Hz, 2H, aromatic H, benzyl), 7.68–7.66 (m, 2H, *o*-Ph-*H*, 3-phenyl), 7.54–7.48 (m, 3H, *m*-Ph-*H*, and *p*-Ph-*H*, 3-phenyl), 7.40 (d, $J$ = 7.1 Hz, 2H, aromatic H, benzyl), 5.65 (s, 2H, NHC$H_2$), 4.28 (quartet, $J$ = 6.5 Hz, 2H, $CH_2$), 1.28 ppm (t, $J$ = 6.5 Hz, 3H, $CH_3$); $^{13}$C NMR ([D$_6$]DMSO, 100 MHz): $\delta$ = 165.42, 158.24, 156.13, 154.57, 142.44, 132.71, 129.50, 129.16, 128.76, 128.27, 127.81, 127.42, 113.86, 97.35, 60.74, 49.48, 14.16 ppm; HR-MS (ESI-TOF) (*m/z*): $C_{21}H_{19}N_5O_2$ calcd, 373.1539; found, 374.1649 $[M+H]^+$.

**2-(4-Amino-3-phenyl-1*H*-pyrazolo[3,4-*d*]pyrimidin-1-yl)acetic acid (1).** Compound **16** (225.0 mg, 0.76 mmol) was suspended in a solution of sodium hydroxide (3N, 10.0 mL), dioxane (5.0 mL), and ethanol (5.0 mL). The reaction mixture was refluxed for 2 h, cooled, neutralized with 1N HCl solution, and concentrated under reduced pressure. The residue was dissolved in dichloromethane:methanol (9:1 *v/v*) filtered, concentrated and purified by silica gel column chromatography using dichloromethane and methanol (9:1 *v/v*) as eluents to afford **1** (186 mg, 91%). $^1$H NMR ([D$_6$]DMSO, 400 MHz): $\delta$ = 8.46 (s, 1H, H-6), 7.70–7.68 (m, 2H, *o*-Ph-*H*), 7.59–7.51 (m, 3H, *m*-Ph-*H*, and *p*-Ph-*H*), 5.21 (s, 2H, $CH_2$), 5.20 ppm (br s, 2H, N$H_2$); $^{13}$C NMR ([D$_6$]DMSO, 100 MHz): $\delta$ = 169.70, 156.14, 154.35, 152.49, 146.36, 132.56, 130.56, 130.17, 130.04, 129.06, 97.77, 49.29 ppm; HR-MS (ESI-TOF) (*m/z*): $C_{13}H_{11}N_5O_2$ calcd, 269.0913; found, 270.0257 $[M+H]^+$.

**(±) 2-(4-Amino-3-phenyl-1*H*-pyrazolo[3,4-*d*]pyrimidin-1-yl)propanoic acid (2).** Compound **17** (265.0 mg, 0.85 mmol) was hydrolyzed to **2** (219 mg, 91%) using similar conditions described above for the synthesis of **1**. $^1$H NMR ([D$_6$]DMSO, 400 MHz): $\delta$ = 8.40 (s, 1H, H-6), 7.69–7.68 (m, 2H, *o*-Ph-*H*), 7.59–7.52 (m, 3H, *m*-Ph-*H*, and *p*-Ph-*H*), 5.60 (quartet, $J$ = 7.3 Hz, 1H, C*H*), 2.50 (s, 2H, N$H_2$), 1.77 ppm (d, $J$ = 7.3 Hz, 3H, $CH_3$). $^{13}$C NMR ([D$_6$]DMSO, 100 MHz): $\delta$ = 171.20, 155.65, 153.45, 152.23, 145.03, 132.03, 129.29, 129.01, 128.28, 97.12, 54.58, 16.02 ppm. HR-MS (ESI-TOF) (*m/z*): $C_{14}H_{13}N_5O_2$ calcd, 283.1069; found, 284.2349 $[M+H]^+$.

**3-(4-Amino-3-phenyl-1*H*-pyrazolo[3,4-*d*]pyrimidin-1-yl)propanoic acid (3).** Compound **18** (245.0 mg, 0.79 mmol) was hydrolyzed to **3** (210 mg, 94%) using similar conditions described above for the synthesis of **1**. $^1$H NMR ([D$_6$]DMSO, 400 MHz): $\delta$ = 8.24 (s, 1H, H-6), 7.63–7.61 (m, 2H, *o*-Ph-*H*), 7.54–7.45 (m, 3H, *m*-Ph-*H*, and *p*-Ph-*H*), 4.52 (t, $J$ = 7.2 Hz, 2H, N$CH_2$), 2.71 ppm (t, $J$ = 7.2 Hz, 2H $CH_2$CO); $^{13}$C NMR ([D$_6$]DMSO, 100 MHz): $\delta$ = 174.47, 158.90, 157.11, 156.23, 143.88, 134.09, 129.94, 129.33, 129.09, 69.90, 51.13, 40.94, 23.58 ppm; HR-MS (ESI-TOF) (*m/z*): $C_{14}H_{13}N_5O_2$ calcd, 283.1069; found, 284.2789 $[M+H]^+$.

**4-(4-Amino-3-phenyl-1*H*-pyrazolo[3,4-*d*]pyrimidin-1-yl)butanoic acid (4).** Compound **19** (230.0 mg, 0.74 mmol) was hydrolyzed to **4** (195 mg, 89%) using similar conditions described above for the synthesis of **1**. $^1$H NMR ([D$_6$]DMSO, 400 MHz): $\delta$ = 12.00 (1H, COO*H*), 8.24 (s, 1H, H-6), 7.67 (dd, m, 2H, *o*-Ph-*H*), 7.56–7.48 (m, 3H, *m*-Ph-*H*, and *p*-Ph-*H*), 4.36 (t, $J$ = 6.8 Hz, 2H, N$CH_2$), 2.17 (t, $J$ = 6.8 Hz, 2H, $CH_2$CO), 2.04 ppm (quintet, $J$ = 6.8 Hz, 2H, -$CH_2CH_2CH_2$); $^{13}$C NMR ([D$_6$]DMSO, 100 MHz): $\delta$ = 174.71, 158.14, 155.72, 154.17, 143.50, 132.99, 129.15, 128.61, 128.24, 45.99, 32.08, 25.23 ppm; HR-MS (ESI-TOF) (*m/z*): $C_{15}H_{15}N_5O_2$ calcd, 297.1226; found, 298.2532 $[M+H]^+$.

**(±) 3-(4-Amino-3-phenyl-1*H*-pyrazolo[3,4-*d*]pyrimidin-1-yl)butanoic acid (5).** Compound **20** (275.0 mg, 0.88 mmol) was hydrolyzed to **5** (242 mg, 92%) using similar conditions described above for the synthesis of **1**. $^1$H NMR ([D$_6$]DMSO, 400 MHz): $\delta$ = 8.24 (s, 1H, H-6), 7.69–7.62 (m, 2H, *o*-Ph-*H*), 7.61–7.50 (m, 3H, *m*-Ph-*H*, and *p*-Ph-*H*), 4.78 (m, 1H, NC*H*), 2.26 (d, $J$ = 6.7 Hz, 2H, $CH_2$CO), 1.04 ppm (d,

  

$J$ = 6.7 Hz, 3H, -CH(C$H_3$); $^{13}$C NMR ([D$_6$]DMSO, 100 MHz): $\delta$ = 174.45, 158.90, 157.11, 156.23, 143.87, 134.09, 129.94, 129.32, 129.08, 128.25, 114.69, 69.89, 43.78, 31.58, 23.57 ppm; HR-MS (ESI-TOF) (*m/z*): $C_{15}H_{15}N_5O_2$ calcd, 297.1226; found, 298.2622[*M*+H]$^+$.

**4-((4-Amino-3-phenyl-1*H*-pyrazolo[3,4-*d*]pyrimidin-1-yl)methyl)-benzoic acid (6).** Compound **21** (300.0 mg, 0.80 mmol) was hydrolyzed to **6** (256 mg, 93%) using similar conditions described above for the synthesis of **1**. $^1$H NMR ([D$_6$]DMSO, 400 MHz): $\delta$ = 8.29 (s, 1H, H-6), 7.89 (d, $J$ = 8.1 Hz, 2H, aromatic H, benzyl), 7.68 (m, 2H, *o*-Ph-*H*, 3-phenyl), 7.59–7.41 (m, 3H, *m*-Ph-*H*, and *p*-Ph-*H*, 3-phenyl), 7.36 (d, $J$ = 8.1 Hz, 2H, aromatic H, benzyl), 5.48 ppm (s, 2H, C$H_2$); $^{13}$C NMR ([D$_6$]DMSO, 100 MHz): $\delta$ = 167.13, 158.24, 156.13, 154.53, 141.71, 132.73, 129.77, 129.65, 129.17, 128.76, 128.27, 127.57, 49.53 ppm; HR-MS (ESI-TOF) (*m/z*): $C_{19}H_{15}N_5O_2$ calcd, 345.1226; found, 346.2234[*M*+H]$^+$.

**PhPP-CH$_2$CONH-CIYKYY (25).** The peptide CIYKYY was assembled on Fmoc-Tyr(*t*Bu)-Wang resin (115.0 mg, 0.88 mmol/g) by Fmoc solid-phase peptide synthesis strategy using Fmoc protected amino acids [Fmoc-Tyr(*t*Bu)-OH (Y$^5$), Fmoc-Lys(Boc)-OH (K$^4$), Fmoc-Tyr(*t*Bu)-OH (Y$^3$), Fmoc-Ile-OH (I$^2$), and Fmoc-Cys(Trt)-OH (C$^1$)] on a PS3 automated peptide synthesizer at room temperature. The Fmoc protecting group was removed with piperidine in DMF (twice, 20%, 25 mL) by shaking at room temperature for 10 min. The resin was collected by filtration and washed with DMF (2× 20 mL), MeOH (2×20 mL), and DCM (2×20 mL), respectively, and dried under vacuum. The free amino group was coupled with PhPPCH$_2$COOH (**1**, 58 mg, 0.22 mmol) in the presence of HBTU (174 mg, 0.46 mmol) and DIPEA (99%, 81 μL, 0.46 mmol) in DMF (20 mL) by shaking at room temperature for 6 h. The resin was collected by filtration and washed with DMF (2×20 mL) and DCM (2× 20 mL) and dried under vacuum. The synthesized compound was cleaved and deprotected from the resin by shaking it with a mixture of TFA:anisole:water:EDT (95:2.0:2.0:1.0 *v/v/v/v*, 5.0 mL) for 1 h. The crude compound was precipitated by the addition of cold diethyl ether (25 mL, Et$_2$O) and purified by preparative HPLC to afford **25**. $^1$H NMR ([D$_6$]DMSO, 400 MHz): $\delta$ = 9.40–9.05 (m, 2H), 8.40–8.10 (m, 4H), 8.05–7.75 (m, 4H), 7.70–7.60 (m, 1H), 7.59–7.48 (m, 2H), 7.10–6.95 (m, 6H), 6.70–6.58 (m, 6H), 5.01 (s, 1H), 4.60–4.01 (m, 7H), 3.15–2.60 (m, 15H), 1.90–1.80 (m, 4H), 1.65–0.60 ppm (m, 11H); HR-MS (ESI-TOF) (*m/z*): $C_{55}H_{66}N_{12}O_{11}S$ calcd, 1102.4695; found, 1103.5427 [M + H]$^+$, 552.0639 [*M*+2H]$^{2+}$.

**Radioactive kinase assay.** The inhibitory potencies of the synthesized compounds against active c-Src were examined using a radioactive kinase assay with polyE$_4$Y (average MW: 35kD) as an artificial substrate. Active p60-c-Src was purchased from Upstate Cell Signaling. The inhibitory potency of the compounds was determined using a standard radiometric PTK activity assay. The assays were performed using protein kinase assay buffer (HEPES pH 8, 5% glycerol, 0.005% Triton X-100, 0.05% β-mercaptoethanol) containing poly(E$_4$Y) (1 mg mL$^{-1}$), as the phosphate-accepting substrate, [γ-$^{32}$P]-ATP, ATP (200 μM), and MgCl$_2$ (12 mM). β-Mercaptoethanol blocks the oxidation of cysteine under the assay conditions. After a reaction time of 30 min at 30 °C, 35 μL of the reaction mixture was removed and spotted onto a filter paper and placed into warm 5% trichloroacetic acid (TCA). The TCA stops the kinase reaction, precipitates the proteins and poly-E$_4$Y onto the filter paper, and washes the unreacted ATP and others away. After three TCA washes for 10 min each, the radioactivity remaining on the filter paper was determined by liquid scintillation counting. The assays were done in duplicates and repeated at least three times. Control reactions lacking polyE$_4$Y were included for each enzyme concentration to correct for any nonpolyE$_4$Y-specific phosphorylation. The percentage of inhibition was plotted as a function of the compound. The concentration and the IC$_{50}$ values (the concentration of a compound that caused 50% inhibition) were obtained from such a plot.

The steady-state kinetic assay with active Src was carried out using a radioactive assay to evaluate mechanisms of inhibition by peptide **25** relative to natural substrate ATP. To determine the inhibitory mechanism with regard to ATP, the $K_m$ and $V_m$ values with ATP as the variable substrate was determined at various concentrations of **25**, whereas other components of the assay were at fixed concentrations using Lineweaver double reciprocal plots. The inhibitory mechanism was determined on the basis of the effect of the compound on the $K_m$ and $V_m$ values. The inhibitory constant ($K_i$) was determined by using the SigmaPlot 8.0 Enzyme Kinetics Module.

**Molecular Modeling.** Simulations were performed with the Accelrys Insight II 2000/Discover 97 modeling package, with the cff91 force field. Model of PP1 bound to Src (Figure 5a) was constructed based on the X-ray crystal structures of PP1 bound to Hck (1QCF)[19] and AMP-PNP bound to c-Src (2SRC)[54] templates from RCSB Protein Data Bank. The coordinates and positions of the backbone atoms of PP1 was superimposed on the corresponding atoms in AMP-PNP after which Hck was deleted. During minimization, all atoms were held fixed except for PP1 and binding site residues within 8 Å of PP1. For refinement, the PP1–Src complex first underwent 50 steps of steepest descent and 150 steps of conjugate gradient minimization. Next, the complex was equilibrated briefly with ten molecular dynamics runs of 200 steps each at 300 K. Velocities were reassigned to a random Boltzmann distribution for each run. The final structure was then minimized for 300 steps with the conjugate gradient algorithm. For the molecular modeling of PhPP–CH$_2$COOH (Figure 5b) and PhPP–peptide conjugates (Figure 6 and 7), after initial minimization, the coordinates and positions of the backbone atoms of PhPP in the conjugate was superimposed on the corresponding atoms in PP1 in complex with c-Src after which PP1 was deleted. The minimization was carried out as described above.

## Acknowledgements

*We acknowledge the financial support from the American Cancer Society (RSG CDD-106966).*

**Keywords:** peptides · pyrazolopyrimidine · solid-phase synthesis · Src kinase · structure–activity relationships

[1] S. R. Hubbard, J. H. Till, *Annu. Rev. Biochem.* **2000**, *69*, 373–398.
[2] M. Warmuth, R. Damoiseaux, Y. Liu, D. Fabbro, N. Gray, *Curr. Pharm. Des.* **2003**, *9*, 2043–2059.
[3] M. Susa, A. Teti, *Drug News Perspect.* **2000**, *13*, 169–175.
[4] S. M. Thomas, J. S. Brugge, *Annu. Rev. Cell Dev. Biol.* **1997**, *13*, 513–609.
[5] J. S. Biscardi, D. A. Tice, S. J. Parsons, *Adv. Cancer Res.* **1999**, *76*, 61–119.
[6] T. J. Yeatman, *Nat. Rev. Cancer* **2004**, *4*, 470–480.
[7] D. W. Owens, G. W. McLean, A. W. Wyke, C. Paraskeva, E. K. Parkinson, M. C. Frame, V. G. Brunton, *Mol. Biol. Cell* **2000**, *11*, 51–64.
[8] G. S. Martin, *Nat. Rev. Mol. Cell Biol.* **2001**, *2*, 467–475.
[9] J. D. Bjorge, A. Jakymiw, D. J. Fujita, *Oncogene* **2000**, *19*, 5620–5635.
[10] T. Sawyer, B. Boyce, D. Dalgarno, J. Luliucci, *Expert Opin. Invest. Drugs* **2001**, *10*, 1327–1344.
[11] P. Soriano, C. Montgomery, R. Geske, A. Bradley, *Cell* **1991**, *64*, 693–702.
[12] R. B. Irby, T. J. Yeatman, *Oncogene* **2000**, *19*, 5636–5642.
[13] R. J. Budde, S. Ke, V. A. Levin, *Cancer Biochem. Biophys.* **1994**, *14*, 171–175.
[14] W. Mao, R. Irby, D. Coppola, L. Fu, M. Wloch, J. Turner, H. Yu, R. Garcia, R. Jove, T. J. Yeatman, *Oncogene* **1997**, *15*, 3083–3090.

  

[15] B. P. Eliceiri, R. Paul, P. L. Schwartzberg, J. D. Hood, J. Leng, D. A. Cheresh, *Mol. Cell* **1999**, *4*, 915 – 924.
[16] R. Paul, Z. G. Zhang, B. P. Eliceiri, Q. Jiang, A. D. Boccia, R. L. Zhang, M. Chopp, D. A. Cheresh, *Nat. Med.* **2001**, *7*, 222 – 227.
[17] K. Parang, G. Sun, *Expert Opin. Ther. Pat.* **2005**, *15*, 1183 – 1207.
[18] K. Parang, G. Sun, *Curr. Opin. Drug Discov. Devel.* **2004**, *7*, 630 – 638.
[19] T. Schindler, F. Sicheri, A. Pico, A. Gazit, A. Levitzki, J. Kuriyan, *Mol. Cell* **1999**, *3*, 639 – 648.
[20] F. Sicheri, I. Moarefi, J. Kuriyan, *Nature* **1997**, *385*, 602 – 610.
[21] S. S. Taylor, E. Radzio-Andzelm, *Structure* **1994**, *2*, 345 – 355.
[22] K. Parang, P. A. Cole, *Pharmacol. Ther.* **2002**, *2–3*, 145 – 157.
[23] M. Y. Yoon, P. F. Cook, *Biochemistry* **1987**, *26*, 4118 – 4125.
[24] U. Schulze-Gahmen, J. Brandsen, H. D. Jones, D. O. Morgan, L. Meijer, J. Vesely, S. H. Kim, *Proteins Struct. Funct. Genet.* **1995**, *22*, 378 – 391.
[25] X. Zhu, J. L. Kim, J. R. Newcomb, P. E. Rose, D. R. Stover, L. M. Toledo, H. Zhao, K. A. Morgenstern, *Struct. Fold Des.* **1999**, *7*, 651 – 661.
[26] L. M. Toledo, N. B. Lydon, D. Elbaum, *Curr. Med. Chem.* **1999**, *6*, 775 – 805.
[27] S. Schenone, O. Bruno, A. Ranise, F. Bondavalli, C. Brullo, P. Fossa, L. Mosti, G. Menozzi, F. Carraro, A. Naldini, C. Bernini, F. Manetti, M. Botta, *Bioorg. Med. Chem. Lett.* **2004**, *14*, 2511 – 2517.
[28] R. J. Budde, N. U. Obeyesekere, S. Ke, J. S. McMurray, *Biochim. Biophy. Acta* **1995**, *1248*, 50 – 56.
[29] J. R. Kamath, R. Liu, A. M. Enstrom, Q. Lou, K. S. Lam, *J. Pept. Res.* **2003**, *62*, 260 – 268.
[30] K. S. Lam, J. Wu, Q. Lou, *Int. J. Pept. Protein Res.* **1995**, *45*, 587 – 592.
[31] Z. Songyang, K. L. 3rd Carraway, M. J. Eck, S. C. Harrison, R. A. Feldman, M. Mohammadi, J. Schlessinger, S. R. Hubbard, D. P. Smith, C. Eng, M. J. Lorenzo, B. A. J. Ponder, B. J. Mayer, L. C. Cantley, *Nature* **1995**, *373*, 536 – 539.
[32] Q. Lou, M. E. Leftwich, K. S. Lam, *Bioorg. Med. Chem.* **1996**, *4*, 677 – 682.
[33] L. Tatton, G. M. Molrey, R. Chopra, A. Khwaja, *J. Biol. Chem.* **2003**, *278*, 4847 – 4853.
[34] J. F. Dorsey, R. Jove, A. J. Kraker, J. Wu, *Cancer Res.* **2000**, *60*, 3127 – 3131.
[35] R. Sundaramoorthi, W. C. Shakespeare, T. P. Keenan, C. A. Metcalf, Y. Wang, U. Mani, M. Taylor, S. Liu, R. S. Bohacek, S. S. Narula, D. C. Dalgarno, M. R. Van Schravandijk, S. M. Violette, S. Liou, S. Adams, M. K. Ram, J. A. Keats, M. Weigele, T. K. Sawyer, *Bioorg. Med. Chem. Lett.* **2003**, *13*, 3063 – 3066.
[36] J. H. Hanke, J. P. Gardner, R. L. Dow, P. S. Changelian, W. H. Brissette, E. J. Weringer, B. A. Pollok, P. A. Connelly, *J. Biol. Chem.* **1996**, *271*, 695 – 701.
[37] J. Bain, H. M. McLauchlan, E. P. Cohen, *Biochem. J.* **2003**, *371*, 199 – 204.
[38] J. Alfaro-Lopez, W. Yuan, B. C. Phan, J. Kamath, Q. Lou, K. S. Lam, V. J. Hruby, *J. Med. Chem.* **1998**, *41*, 2252 – 2260.
[39] A. Kumar, G. Ye, Y. Wang, X. Lin, G. Sun, K. Parang, *J. Med. Chem.* **2006**, *49*, 3395 – 3401.
[40] K. Parang, J. H. Till, A. J. Ablooglu, R. A. Kohanski, S. R. Hubbard, P. A. Cole, *Nat. Struct. Biol.* **2001**, *8*, 37 – 41.
[41] N. H. Nam, S. Lee, G. Ye, G. Sun, K. Parang, *Bioorg. Med. Chem.* **2004**, *12*, 5753 – 5766.
[42] U. Hanefeld, C. W. Rees, A. J. P. White, D. J. Williams, *J. Chem. Soc. Perkin Trans. 1* **1996**, 1545 – 1552.
[43] A. F. Burchat, D. J. Calderwood, M. M. Friedman, G. C. Hirst, B. Li, P. Rafferty, K. Ritter, B. S. Skinner, *Bioorg. Med. Chem. Lett.* **2002**, *12*, 1687 – 1690.
[44] N. H. Nam, R. Pitts, G. Sun, S. Sardari, A. Tiemo, M. Xie, B. Yan, K. Parang, *Bioorg. Med. Chem.* **2004**, *12*, 779 – 787.
[45] N.-H. Nam, G. Ye, G. Sun, K. Parang, *J. Med. Chem.* **2004**, *47*, 3131 – 3141.
[46] T. Tanoue, E. Nishida, *Pharmacol. Ther.* **2002**, *93*, 193 – 202.
[47] D. Wang, X. Y. Huang, P. A. Cole, *Biochemistry* **2001**, *40*, 2004 – 2010.
[48] S. Lee, X. Lin, N. H. Nam, K. Parang, G. Sun, *Proc. Natl. Acad. Sci. USA* **2003**, *100*, 14707 – 14712.
[49] S. Lee, M. K. Ayrapetov, D. Kemble, K. Parang, G. Sun, *J. Biol. Chem.* **2006**, *281*, 8183 – 8189.
[50] A. C. Bishop, K. Shah, Y. Liu, L. Witucki, C. Kung, K. M. Shokat, *Curr. Biol.* **1998**, *8*, 257 – 262.
[51] K. Shah, Y. Liu, C. Deirmengian, K. M. Shokat, *Proc. Natl. Acad. Sci. USA* **1997**, *94*, 3565 – 3570.
[52] Y. Liu, K. Shah, F. Yang, L. Witucki, K. M. Shokat, *Bioorg. Med. Chem.* **1998**, *6*, 1219 – 1226.
[53] Y. Liu, K. Shah, F. Yang, L. Witucki, K. M. Shokat, *Chem. Biol.* **1998**, *5*, 91 – 101.
[54] W. Xu, A. Doshi, M. Lei, M. J. Eck, S. C. Harrison, *Mol. Cell* **1999**, *3*, 629 – 638.
[55] B. T. Houseman, J. H. Huh, S. J. Kron, M. Mrksich, *Nat. Biotechnol.* **2002**, *20*, 270 – 274.
[56] R. Karni, S. Mizrachi, E. Reiss-Sklan, A. Gazit, O. Livnah, A. Levitzki, *FEBS Lett.* **2003**, *537*, 47 – 52.

Received: March 30, 2007
Revised: April 28, 2007
Published online on May 25, 2007

  